

Defects tracking in Out-of-Autoclave composite materials

MARIANA DA GAMA E CASTRO MOURA SOARES

Supervisor:

Prof. Dr. António Torres Marques

A Thesis submitted to the Faculty of Engineering, University of Porto
in partial fulfillment of the requirements for the degree of
Master of Science in Mechanical Engineering

Porto, September 2017

*“I may not have gone where I intended to go, but I
think I have ended up where I needed to be.”*

— Douglas Adams

Abstract

Keywords: Composites, Curing Process, Out-of-Autoclave, Finite Element Analysis (FEA).

Advanced thermosetting carbon fibre reinforced polymers (CFRP) have become common in primary aerospace structures, along with high performance sporting goods and marine and wind energy structures. As these composite parts grow in number, size and complexity, the need for faster, more cost effective and more versatile manufacturing comes into conflict with the limitations of traditional processing methods.

The cure of the resin is a process phase of utmost importance in vacuum bag only (VBO) and resin transfer moulding (RTM) processes, as it is for composite manufacturing processes in general. The result of the curing process determines the quality of a part due to its great influence on mechanical and chemical properties and life cycle of the part under high temperature. Therefore, the discussion of the curing process is of tremendous importance and value.

In the cure of a thermoset fibre-reinforced composite laminate, stress and strain develop as the matrix resin undergoes crosslinking reactions accompanied by chemically induced volumetric shrinkage. In addition to this cure-induced effect, thermal deformation occurs during the subsequent cooling. Consequent residual stress and strain can cause shape distortion and premature failure of the cured composite. Therefore, cure process optimization is important and costly trial-and-error methods are often necessary to set appropriate tool geometry and cure cycle.

In the present work, a computational analysis of the curing process of a specific part is performed in two different softwares. Three distinct materials, (AS4/8552, IM7/5250-1 and a non-crimped fabric composed by HTS fibres and RTM6 epoxy matrix) each corresponding to a different manufacturing process, are analysed. Firstly, using Raven[®] and with an adequate application of boundary conditions, it is possible to obtain the value of the heat transfer coefficient that cures the composite laminate part and generates a laminate and mould temperature distribution that follow the curing temperature. Secondly, a finite element model is generated and, using the results from Raven[®], it is possible to obtain the strain gradient of the part in study and consequently, possible locations for defects to occur in the composite laminated part.

Resumo

Palavras-chave: Compósitos, Processo de cura, Fora-de-autoclave, Análise de Elementos Finitos (AEF).

Os Polímeros Reforçados com Fibra de Carbono (PRFC) tornaram-se uma matéria-prima comum na indústria aeroespacial, assim como no fabrico de bens desportivos de alta performance e de estruturas para obtenção de energia, tanto marinhas como eólicas. Com o crescimento da utilização de peças fabricadas em materiais compósitos surgiu a necessidade de produzir peças maiores e mais complexas e, consequentemente, a necessidade de um fabrico mais rápido, rentável e versátil, o que deixou de ser possível obter através de processos de fabrico tradicionais.

Uma fase de extrema importância tanto no processo VBO como no RTM é a fase da cura da resina. O resultado do processo de cura da resina determina a qualidade da peça fabricada, influencia as propriedades mecânicas, o ciclo de vida da peça a elevadas temperaturas e as propriedades químicas, sendo de extrema importância a discussão e estudo do processo de cura no fabrico de uma peça em material compósito.

Na cura de um compósito laminado de resina termoendurecível reforçada com fibra, as tensões e deformações desenvolvem-se de acordo com as reações de ligação cruzadas sofridas pela matriz de resina e com o encolhimento volumétrico induzido quimicamente. Para além deste efeito da cura, ocorre deformação térmica na fase de arrefecimento subsequente, o que provoca o aparecimento de tensões e deformações residuais que podem causar deformações na geometria da peça e uma rutura prematura na peça curada. Desta forma, a otimização do processo de cura torna-se de importância imperativa, sendo muitas vezes necessários métodos de tentativa e erro caros, de forma a determinar a geometria do molde e o ciclo de cura mais apropriados.

No presente trabalho, é feita uma análise computacional do processo de cura utilizando dois softwares distintos. São analisados três materiais diferentes (AS4/8552, IM7/5250-1 e um tecido *non-crimped* composto por fibras HTS e uma matriz de resina RTM6), cada um correspondente a um diferente processo de fabrico. A simulação é iniciada utilizando o software Raven[®] e aplicando as condições de fronteira adequadas, sendo possível obter o valor do coeficiente de transferência de calor que cura o laminado e que gera a distribuição de temperatura, deste e do molde, que acompanha a temperatura de cura. Seguidamente, é gerado um modelo de elementos finitos e, utilizando os resultados obtidos no Raven[®], é possível obter a distribuição

de tensões na peça e, conseqüentemente, as possíveis localizações para aparecimento de defeitos.

Acknowledgements

I would like to take this opportunity to express my gratitude to my supervisor, Prof. Dr. António Torres Marques, for his availability throughout the time of this work and his effort to make this a theme I would be interested to work on.

I am grateful to Professor Pascal Hubert for taking the time to guide me on the formulation of the approach of the problem and for providing me with a Raven[®] software licence.

To the friends I made during these years at the university, for the joyful and for the tough times spent together. To Ana, Ana, Catarina, Joana, Joana, Pedro e Rafa. To my long time friend Inês for always caring.

To Luís for his support and affection and for his readiness to help, always willing to share his knowledge.

To all my family, in particular to my brother and sister and to my grandparents. And mostly to my parents, without whom this would not be possible, for their unconditional support throughout this journey.

Contents

Abstract	i
Resumo	iii
Acknowledgements	v
List of symbols	ix
List of figures	xi
List of tables	xiv
1 Introduction	1
1.1 Background	1
1.2 Rational	3
1.3 Problem Statement	3
1.4 Objectives	3
1.5 Thesis layout	4
2 State-of-the-art	5
2.1 Composite materials	5
2.2 Manufacturing composite processes	6
2.2.1 Autoclave processing	7
2.2.2 Open moulding processes	9
2.2.3 Closed moulding processes	12
2.3 Curing process	29
2.4 Manufacturing defects	30
2.5 RAVEN [®] simulation software	33
3 Numerical Simulations	37
3.1 Geometry	38
3.2 Materials	39
3.3 Step I - RAVEN [®]	42
3.3.1 Autoclave	42
3.3.2 VBO	45
3.3.3 Results and discussion	48
3.4 Step II - Finite element modelling	49
3.4.1 Autoclave	50
3.4.2 RTM	55

3.4.3	VBO	60
3.5	Discussion	66
4	Conclusions and Future Work	67
4.1	Conclusions	67
4.2	Future work	68
	Bibliography	69
A	ABAQUS[®] 3D computational models	75

List of Symbols

Chapter 2

ϕ	In-plane fibre angle of the FW process;
θ	In-plane fibre angle of the FW process;
w	Total tow width of the FW winding process;
ω	Rotational speed of the mandrel of the FW process;
F	Total force that the tows create in the head of the FW process;
V	Axial velocity of the moving platform of the FW process;
Ca^*	Modified capillary number;
μ	Resin dynamic viscosity;
\bar{u}	Global resin velocity;
γ	Surface tension of resin;
θ	Contact angle between the resin and fibres;
u	Axial displacement in the x direction;

Chapter 3

E_{11}^c	Longitudinal laminate level Young's modulus;
E_{22}^c	Transversal laminate level Young's modulus;
E_{33}^c	Through-thickness laminate level Young's modulus;
ν_{12}^c	In-plane laminate level Poisson's coefficient;
ν_{13}^c	Longitudinal laminate level Poisson's coefficient;
ν_{23}^c	Through-thickness laminate level Poisson's coefficient;
G_{12}^c	In-plane laminate level shear modulus;
G_{13}^c	Longitudinal laminate level shear modulus;
G_{23}^c	Through-thickness laminate level shear modulus;
ρ^c	Laminate level density;
c^c	Laminate level specific heat;
k_{11}^c	Longitudinal laminate level heat conductivity coefficient;
k_{22}^c	Transversal laminate level heat conductivity coefficient;
k_{33}^c	Through-thickness laminate level heat conductivity coefficient;
α_{11}^c	Longitudinal laminate level coefficient of thermal expansion;
α_{22}^c	Transversal laminate level coefficient of thermal expansion;
ω_f	Fibre volume fraction;
E_{11}^f	Fibres longitudinal fibres Young's modulus;
E_{22}^f	Fibres transversal fibres Young's modulus;
ν_{12}^f	Fibres in-plane fibres Poisson's coefficient;

G_{12}^f	Fibres in-plane shear modulus;
ρ^f	Fibres density;
k_{11}^f	Fibres longitudinal heat conductivity coefficient;
k_{22}^f	Fibres transversal heat conductivity coefficient;
α_{11}^f	Fibres longitudinal coefficient of thermal expansion;
α_{22}^f	Fibres transversal coefficient of thermal expansion;
E^m	Matrix Young's modulus;
ν^m	Matrix Poisson's coefficient;
G^m	Matrix shear modulus;
ρ^m	Matrix density;
k^m	Matrix heat conductivity coefficient;
α^m	Matrix coefficient of thermal expansion;
E^I	Invar 36 Young's modulus;
ν^I	Invar 36 Poisson's coefficient;
G^I	Invar 36 shear modulus;
ρ^I	Invar 36 density;
k^I	Invar 36 heat conductivity coefficient;
α^I	Invar 36 coefficient of thermal expansion;
E^s	Stiffener Young's modulus;
ν^s	Stiffener Poisson's coefficient;
G^s	Stiffener shear modulus;
ρ^s	Stiffener density;
k^s	Stiffener heat conductivity coefficient;
α^s	Stiffener coefficient of thermal expansion;
h	Heat transfer coefficient;

List of Figures

2.1	Schematic view of vacuum bagging for autoclave processing [1]. . . .	7
2.2	Schematic view of the set up inside an autoclave and principal of autoclave curing [2].	8
2.3	Schematic view of a typical autoclave device [2].	8
2.4	Schematic view of the hand lay-up process [3].	9
2.5	Schematic view of the spray lay-up process [3].	10
2.6	Schematic view of the FW process [2].	11
2.7	Filament winding patterns [2].	11
2.8	Schematic view of the roll wrapping process [4].	12
2.9	Schematic view of the Compression moulding [5].	13
2.10	Injection moulding cyclic process [6].	15
2.11	General steps of Reaction Injection Moulding (RIM) [7].	16
2.12	General steps of the Vacuum Infusion (VI) process [8].	17
2.13	Schematic view of the resin film infusion process [9].	18
2.14	Schematic view of the Centrifugal Casting process [10].	19
2.15	Schematic view of continuous lamination [10].	19
2.16	Schematic view of the pultrusion process [11].	20
2.17	Schematic view of injected pultrusion [11].	21
2.18	Schematic view of Quickstep TM process [12].	21
2.19	Schematic view of RTM [8].	23
2.20	Schematic view of VARTM process [13].	24
2.21	Schematic view of SCRIMP [14].	25
2.22	Resin injection sequence in the HPIRTM process [15].	26
2.23	Resin injection sequence in the HPCRTM process [15].	26
2.24	Schematic and micrograph of air evacuation channels in VBO prepreg [16].	27
2.25	Schematic of evacuation of entrapped air from VBO prepreg. [11]. .	28
2.26	VBO lay-up schematic [16].	28
2.27	Void formation mechanism in the RTM process [17].	31
2.28	Void content as a function of modified capillary number [17]. . . .	31
2.29	Influence of various process parameters on porosity in VBO compos- ites [16].	32
2.30	1st explanation figure of the RAVEN [®] software.	34
2.31	2nd explanation figure of the RAVEN [®] software.	35
2.32	3rd explanation figure of the RAVEN [®] software.	35
2.33	4th explanation figure of the RAVEN [®] software.	36
2.34	5th explanation figure of the RAVEN [®] software.	36
3.1	Model representation scheme	38

3.2	Laminate parts	39
3.3	Laminate parts	39
3.4	Variation of the CTE with fibre volume fraction for the reported constituents [18, 19, 20, 21].	41
3.5	Autoclave model setup in Raven [®]	43
3.6	Curing temperature distribution of the autoclave model.	43
3.7	Mould and laminate temperature vs curing temperature distribution for the autoclave process for different values of h	44
3.8	Degree of cure of AS4/8552 during curing cycle for $h = 80 \text{ W/m}^2\text{K}$	45
3.9	Cure rate of AS4/8552 during curing cycle, for $h = 80 \text{ W/m}^2\text{K}$	45
3.10	VBO model setup in Raven [®]	46
3.11	Curing temperature distribution of the VBO model.	46
3.12	Mould and laminate temperature vs curing temperature distribution for the VBO process for different values of h	47
3.13	Degree of cure of IM7/5320-1 during curing cycle for $h = 50 \text{ W/m}^2\text{K}$	48
3.14	Cure rate of IM7/5320-1 during curing cycle for $h = 50 \text{ W/m}^2\text{K}$	48
3.15	Autoclave and VBO computational models and evidence of the eight plies.	49
3.16	RTM computational model.	49
3.17	Pressure load distribution applied during curing process in the autoclave model.	50
3.18	Loads and BC applied to the autoclave computational model.	51
3.19	Strain distribution in the first ply after the curing process.	51
3.20	Stress distribution in the first ply after the curing process.	51
3.21	Strain distribution in the second ply after the curing process.	52
3.22	Stress distribution in the second ply after the curing process.	52
3.23	Strain distribution in the third ply after the curing process.	52
3.24	Stress distribution in the third ply after the curing process.	52
3.25	Strain distribution in the fourth ply after the curing process.	53
3.26	Stress distribution in the fourth ply after the curing process.	53
3.27	Strain distribution in the fifth ply after the curing process.	53
3.28	Stress distribution in the fifth ply after the curing process.	53
3.29	Strain distribution in the sixth ply after the curing process.	54
3.30	Stress distribution in the sixth ply after the curing process.	54
3.31	Strain distribution in the seventh ply after the curing process.	54
3.32	Stress distribution in the seventh ply after the curing process.	54
3.33	Strain distribution in the eighth ply after the curing process.	55
3.34	Stress distribution in the eighth ply after the curing process.	55
3.35	RTM 6 cure cycle for composite manufacture [22].	55
3.36	Loads and BC applied to the RTM computational model.	56
3.37	Strain distribution in the first ply after the curing process.	57
3.38	Stress distribution in the first ply after the curing process.	57
3.39	Strain distribution in the second ply after the curing process.	57
3.40	Stress distribution in the second ply after the curing process.	57
3.41	Strain distribution in the thrid ply after the curing process.	58
3.42	Stress distribution in the third ply after the curing process.	58
3.43	Strain distribution in the fourth ply after the curing process.	58
3.44	Stress distribution in the fourth ply after the curing process.	58

3.45	Strain distribution in the fifth ply after the curing process.	59
3.46	Stress distribution in the fifth ply after the curing process.	59
3.47	Strain distribution in the sixth ply after the curing process.	59
3.48	Stress distribution in the sixth ply after the curing process.	59
3.49	Strain distribution in the seventh ply after the curing process.	60
3.50	Stress distribution in the seventh ply after the curing process.	60
3.51	Strain distribution in the eighth ply after the curing process.	60
3.52	Stress distribution in the eighth ply after the curing process.	60
3.53	Loads and BC applied to the VBO computational model.	61
3.54	Strain distribution in the first ply after the curing process.	62
3.55	Stress distribution in the first ply after the curing process.	62
3.56	Strain distribution in the second ply after the curing process.	62
3.57	Stress distribution in the second ply after the curing process.	62
3.58	Strain distribution in the third ply after the curing process.	63
3.59	Stress distribution in the third ply after the curing process.	63
3.60	Strain distribution in the fourth ply after the curing process.	63
3.61	Stress distribution in the fourth ply after the curing process.	63
3.62	Strain distribution in the fifth ply after the curing process.	64
3.63	Stress distribution in the fifth ply after the curing process.	64
3.64	Strain distribution in the sixth ply after the curing process.	64
3.65	Stress distribution in the sixth ply after the curing process.	64
3.66	Strain distribution in the seventh ply after the curing process.	65
3.67	Stress distribution in the seventh ply after the curing process.	65
3.68	Strain distribution in the eighth ply after the curing process.	65
3.69	Stress distribution in the eighth ply after the curing process.	65

List of Tables

3.1	Composite laminated skin material properties [23, 24, 25, 26]	40
3.2	Invar 36 material properties [27]	42
3.3	Stiffener material properties	42

Chapter 1

Introduction

1.1 Background

Advanced composite materials are becoming increasingly used in the critical structures of both civilian and military aircraft, as they often have a higher strength-to-weight ratio compared to conventional materials, higher stiffness, are corrosion resistant and are able to be tailored to meet specific mechanical criteria.

The excellent mechanical properties of fibrous composites have enabled them to be applied to the design of various structures, in which their performance has been closely investigated. However, a variation in some factors, particularly, residual stress, a crucial factor during the forming process, may ultimately affect the performance of the final product [28].

Cure simulation is an effective tool to predict the cure-induced stress/strain in a composite component and to determine an appropriate process in a reasonable manner with minimal trial-and-error. The accuracy of the simulation depends on the chemical curing process. There are two key factors for the accurate simulation. Input of appropriate material parameters is the first, as without accurate input parameters the simulation cannot reproduce the actual internal state of the curing composite; secondly, the validation of the simulation, without which it is impossible to confirm the validity of the approach employed [29].

White and Hahn, were two of the first authors to develop a process model for an autoclave or hot pressing process. Their papers address the issue of understanding how residual stresses develop during processing and how they can be predicted, by developing a process model which can be used to predict the residual stress history during the curing of composite laminates [30] with experimental validation [31]. Costa and Sousa [32] developed a three-dimensional numerical model to simulate and to analyse the mechanisms dealing with resin flow, heat transfer and the cure of thick composite laminates during autoclave processing. It is based on the Darcy law, the convection-diffusion heat equation and appropriate constitutive relations. Ganapathi et al. [33] developed a simulation process that simultaneously accounts for all physical phenomena involved in a composite manufacturing process. It attempts to accomplish this by coupling heat transfer, cure kinetics, rheology, 1-D consolidation and 2-D resin flow within and out of curing laminates in a transient

manner. Abdelal et al. [34] developed an autoclave process model which includes the effect of the thermal and mechanical properties of the contact layer between the part and the tool on the residual stress by applying an FE-Explicit solver. Yoo et al. [28] presented a simulation of the curing of a carbon/epoxy laminate by taking into consideration the phase changes of the epoxy resin and the corresponding material property changes in the laminate. The simple technique for simulating the entire curing process with simple mechanical properties was developed using FEA, which predicted well the overall change in the generated strains in the composite laminate during the curing process. More recently, Sreekantamurthy et al. [35] developed cure process models of composite parts using commercial off-the-shelf software to analyse and understand the cure responses with reference to the known physics of the composite curing process, and to compare the residual strain predictions from the analysis with those measured using fibre optics strain sensors in the laboratory. RAVEN[®] and COMPRO[®] commercial softwares were used to conduct analytical studies on the cure process modelling of composite autoclave curing process.

Trochu et al. [36] benefited as well from the FEM to study in a computational environment the RTM process. They obtained with the computer simulation the resin pressure distribution and the resin front positions. The calculated results for selected mould geometries are compared with experimental observations. Liu et al. [37] presented three simulation features (gate control, venting, and dry spot formation) developed in an existing mould filling simulation code for RTM to address the processing issues encountered during manufacturing. Phelan [38] developed a simulation based on Darcy's law for modelling mould filling in RTM. The simulation uses a new Flow Analysis Network (FAN) technique to predict and track the movement of the free-surface, and a finite element method to solve the governing equation set for each successive flow front location. Tan et al. [39] developed a technique for simulating the RTM process, where its major feature is a computational steering system that enables the user to make changes during the simulation. The computer code developed is suitable for simulating the resin flow inside two-dimensional and three dimensional fibre preforms of arbitrary shapes. Dimitrovová and Faria [40] performed numerical simulations of the mould filling phase of the RTM process by studying different length-scales, namely the micro-scale (constituents level) and the macro-scale (laminate level) by using homogenization techniques. Rouison et al. [41] developed a model that was capable of predicting the cure behaviour of natural fibre composites and to optimize the RTM process to obtain a high degree of cure in a minimum time. The VARTM process was analysed by Govignon et al. [42] by addressing the complex reinforcement deformation behaviour exhibited during this type of process. The authors developed a macro-scale compaction model in conjunction with compaction experiments to replicate reinforcement behaviour during the pre-filling, filling and post-filling stages. The model was implemented into a FE simulation of the infusion of the reinforcement. Palardy et al. [43] incorporated mathematical models into already existing software to simulate low process additives (LPA) behaviour during actual manufacturing. The authors used the PAM-RTM software to study the pre-heating behaviour of a steel RTM mould. Yoo et al. [28] presents the simulation of the curing of a carbon/epoxy laminate by taking into consideration the phase changes of the epoxy resin and the corresponding material property changes in the laminate. Recently, Sreekantamurthy et al. studied the

curing process of laminated panels which involved thermo-kinetic, resin flow compaction and residual strain analysis using commercial softwares and experimental validation by means of optical fibre strain sensing techniques.

Thanks to the recent advances in the computational techniques, it is possible, with the right modelling strategy, to simulate the curing processes for different manufacturing procedures without having to fabricate and test the material to identify the necessary outputs.

1.2 Rational

With the aim of understanding the performance of Out-of-Autoclave (OoA) manufacturing processes, a qualitative comparison is made between these and the autoclave process. For that, numerical results were obtained using a commercial off-the-shelf software that were fed, a posteriori, in a finite element computational framework to evaluate strain concentration localizations.

1.3 Problem Statement

Due to the sophistication of the modelling techniques and to the ever increasing technological power, process computational modelling has been emerging as an accurate and reliable tool to study the mechanical performance of laminated composites. Testing procedures, defects identification and finite element analysis techniques are at the engineers disposal to evaluate and predict the behaviour of composite materials. The analyses and models developed in this thesis are intended to, with the proper inputs, perform a qualitative comparison between autoclave and OoA processes in terms of identification of strain localizations and consequently, possible appearances of defects.

1.4 Objectives

Given the current state-of-the-art in the different available composite materials manufacturing processes and a way of modelling them, this thesis aims to increase the understanding of the performance, in terms of process induced defects of OoA manufacturing processes, emphasizing Resin Transfer Moulding (RTM) and Vacuum Bag Only (VBO).

The analysis of the process behaviour of a particular multi-directional composite laminate part is one of the major objectives of this thesis. After understanding the different manufacturing processes, curing processes and possible manufacturing defects, a computational Finite Element Model (FEM) was developed. It is able to represent the process conditions of both VBO and RTM manufacturing processes, in order to compare their performance by looking at the formation of defects and evaluating the curing cycles.

1.5 Thesis layout

Chapter 2 presents the state-of-the-art in, generally speaking, composite materials and their different manufacturing processes. It is also addressed, later in the chapter, what type of manufacturing defects can occur in a composite laminated part, the different existing curing cycles for these processes and a simple description regarding the commercial software that was used.

Chapter 3 presents the numerical simulations of the three different manufacturing processes. It involves the full description of the geometry of the generated parts, the materials used for each part and, finally, the numerical results.

Lastly, in Chapter 4, the main conclusions regarding the work carried out during the thesis are presented and some follow-up work for more detailed study of modelling the curing process of laminated composites and defects tracking is proposed.

Chapter 2

State-of-the-art

2.1 Composite materials

Composite materials are replacing standard engineering metals and alloys for many applications and are typically designed with a particular use in mind, such as added strength, efficiency or durability. Fibre-reinforced polymers, for their inherent ability to be custom tailored for an application, are a very viable material option. Their superior specific strength, stiffness and thermal characteristics have made them very competitive in the aerospace industry.

A composite material is, in its general definition, an aggregation of two or more materials combined to obtain a set of properties superior than those of its constituents alone. However, depending on the type of matrix or fibre, some individual properties of the constituents are only transferred as a small fraction to the composite itself, e.g., the mode I interlaminar fracture toughness [44].

Fibre-reinforced plastics (FRP) make up a significant portion of the composites that are used by modern society. FRP can be divided roughly into two groups: synthetic materials reinforced with short fibres, and synthetic materials reinforced with long (continuous) fibres. Composites reinforced with short fibres are used primarily for injection moulding or extruded plastic products. However, composites reinforced with long or continuous fibres are often used in large structures such as ships, pressure tanks, aircrafts and wind turbine wings.

In a fibre-reinforced composite materials, the constituents differ from each other in a molecular level and are mechanically separable. While the fibres convey structural stiffness and strength to FRP materials, the matrix transfers the load between the fibres, with respect to possible external loads, and supports them under compression loading. Strength, stiffness and moduli properties of composites are a function of the Fibre Volume Fraction (FVF) in the section of the FRP.

Commonly, a composite material is formed by a synthetic resin reinforced by high strength fibres. The resin used can be either a thermoplastic, which can be formed and reformed by heat, or a thermoset, which is hardened by a chemical reaction and cannot be reformed. Each material has its place in the market. In broad generalities, thermosets have been around for a long time (have a well-established

place in the market), frequently have lower raw material costs, and often provide easy wetting of the reinforcing fibre and easy forming to final part geometries (are easier to process). Thermoplastics tend to be tougher (less brittle), can have better chemical resistance, don't need refrigeration (as uncured thermosets frequently do), and are more easily recycled and repaired.

The consumption of plastics is increasing every year and the rise of virgin plastic prices made the plastic product manufacturers or consumers look for alternative resources to survive in a competitive business market, which made recycled plastics a promising solution. Several Life Cycle Analysis (LCA) for composite applications have been carried out and reported [45]. A brief and important conclusion regarding this thematic was observed by Rajendran et al. [46], where it was concluded that the use of recycled plastics for a composite application can have a clear environmental advantage over conventional virgin polymers in certain cases. These results are best for civil and infrastructural applications, due to their significant potential to lower the environmental impact. The impact of recycled composites on automotive applications is, at its best, equivalent to that of virgin composites. However, a slight reduction or variation in the properties of plastic waste feed stock could drastically raise the environmental impact several times than that of the virgin alternatives. Hence, in automotive sector applications, substituting or replacing the virgin plastic component with a recycled plastic component is not advisable unless significant weight reductions are obtained at equivalent functional performance.

On a different thematic, one of the most common ways to manufacture composite materials is known as autoclave processing. This process is robust and well-understood, having benefited from significant research and experience gained from widespread industrial use, and remains a benchmark for competing processes. However, autoclaves involve significant costs for acquisition, operation, and tooling, particularly for large parts [16]. This thesis is focused on Resin Transfer Moulding (RTM) and Vacuum Bag Only (VBO) manufacturing processes, which have gained acceptance over the past decade because of their ability to produce autoclave-quality components and even eliminate some defects present on autoclave manufactured materials.

2.2 Manufacturing composite processes

Many different manufacturing processes have evolved to fabricate polymer matrix composites. They were modified or developed to address various needs such as new fibre or matrix systems, new and improved initial precursor material forms, composite part geometrical constraints, cost-effectiveness, multi-functionality of the part, enhancement of a specific physical, electric or mechanical property and defect constraints [11].

In this chapter, a review concerning the different types of manufacturing processes of composite materials is addressed, focusing on those most commonly used in the composite manufacturing industry and utilizing thermoset polymers.

Both autoclave and out-of-autoclave processes are outlined, been an emphasis given to the processes of RTM and VBO.

2.2.1 Autoclave processing

Autoclave processing, also known as prepreg lay-up process, is one of the oldest and most widely used processing method for high-performance composite materials, such as the ones used in the aerospace industry. It is also one of the most developed composite material manufacturing processes and can be used to manufacture thermoplastic or thermoset matrix composites.

Using this technique, prepregs, thin layers of high modulus fibre impregnated with partially cured resin, are cut and stacked to form a component of desired shape. In addition to uncured prepreg, laminated composite structures might also include such materials as honeycomb core, pre-cured composite stiffeners and structural adhesives to bond together the various parts [11]. After assembly, the structure is covered with various layers of cloth (bleeder and breather) and sealed inside a vacuum bag, as illustrated in Figure 2.1. Bleeders assist in achieving an optimal fibre volume fraction by absorbing excess resin and breathers provide a path for removal of air and volatile gasses from the part during cure. In the early days, after lay-up, an important step of the process was the debulking. In this step, after the lay-up of each four layers, entrapped air was squeezed out either by using vacuum bagging or a debulk table. Debulking step was essential because, once the laminate lay-up process is completed, it is almost impossible to remove entrapped air between every two layers. This additional step usually led to extended lay-up time, hence this tool dead time played a significant role in increasing operational cost [47]. Nowadays, with the vacuum of the assembly and the pressure of the autoclave, entrapped air is almost completely removed.

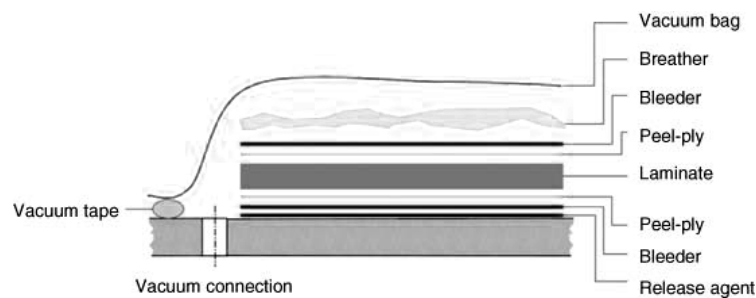


Figure 2.1: Schematic view of vacuum bagging for autoclave processing [1].

The tool-laminate assembly is placed in an autoclave, a device that can generate a controlled pressure and temperature environment, and the bag is connected to the vacuum system. Pressure and temperature are applied to the laminate in order to cure the part (Figure 2.2) in a predetermined cure cycle. The temperature cycle is necessary to trigger the resin polymerization reaction. The pressure is applied to the laminate to conform the laminate to the tool surface and to compact the laminate at the desired fibre volume fraction, and to collapse any voids that may develop during

the resin cure. The bag pressure is controlled to initially remove any entrapped air during lay-up and volatiles during cure. It must be less than the autoclave pressure to ensure compaction of the laminate [11].

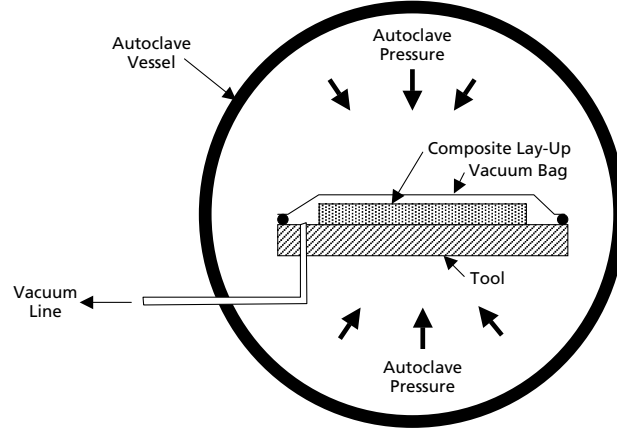


Figure 2.2: Schematic view of the set up inside an autoclave and principal of autoclave curing [2].

The usual procedure for autoclave processing is increasing the pressure before increasing the temperature. Once the pressure reaches its desired limit, it is kept constant throughout the process. As the temperature rises, the resin viscosity drops, thus facilitating the flow and the wetting out of the fibre. The resin viscosity then increases due to polymerization reaction and the wetting process continues till the gelation of resin occurs. The high pressure application assists in proper consolidation and void removal in the product during the wetting process. Once the gelation occurs, the consolidation process stops [48]. Finally, the cured part is debagged and ready for secondary and finishing processes [11].

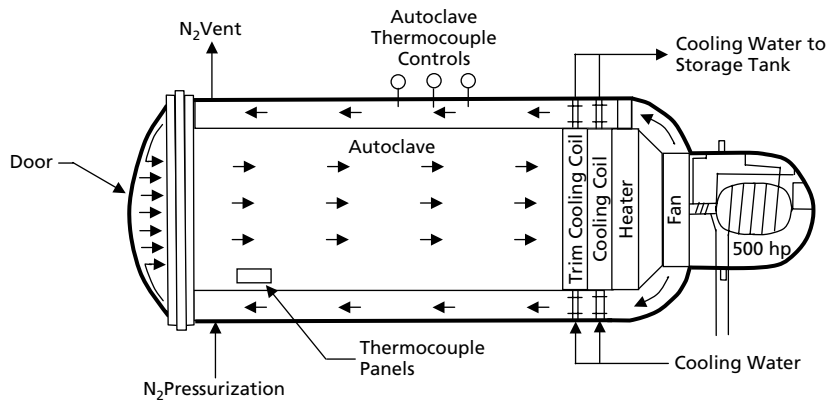


Figure 2.3: Schematic view of a typical autoclave device [2].

A typical autoclave system, shown in Figure 2.3, consists of a pressure vessel, a control system, an electrical system, a gas generation system and a vacuum system.

Autoclaves lend considerable versatility to the manufacturing process. They

can accommodate a single large composite part, such as a large wing skin, or numerous smaller parts loaded onto racks and cured as a batch. Since the gas pressure is applied isostatically to the part, almost any shape can be cured in an autoclave. The only limitation is the size of the device [2].

2.2.2 Open moulding processes

In open moulding processes, raw materials are exposed to air as they cure or harden. These processes still dominate many areas of the composites industry due to its advantages such as being a particularly adaptable method of manufacturing composite components of all shapes, sizes and complexity for relatively little capital investment and only needing one mould. On the other hand, open mould processes have concerns for styrene emissions, which can potentially expose the composite manufacturing workforce to unhealthy levels of styrene. Health and safety regulations, which would virtually eliminate all open moulding processes, are expected [49].

Hand Lay-up

Hand lay-up process, also known as wet lay-up, was the dominant manufacturing method for composite parts in the early days of their usage. Nowadays, it is still very commonly used for being the least expensive open moulding method as it involves the least amount of equipment and does not require high expertise, despite of the intensive labour.

This method is suitable for making a high variety of composite products, from very small to very large. It is widely used in the marine industry and to make prototype parts. It is also the most commonly elected process for making wind-mill blades, storage tanks, swimming pools, tubs and showers [10].

In hand lay-up, the first step is applying gel coat to the mould using a spray gun for a high-quality finish on the visible surface and easier demoulding. When the gel coat has cured, the reinforcement is manually placed on the mould and then impregnated with resin by pouring, brushing or using a paint roller [5]. Fibre reinforced polymer rollers, paint rollers, or squeegees are used to consolidate the laminate, thoroughly wetting the reinforcement and removing entrapped air.

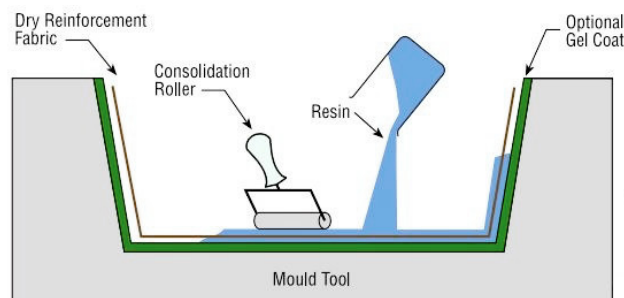


Figure 2.4: Schematic view of the hand lay-up process [3].

Figure 2.4 illustrates the hand lay-up process. The thickness of the composite part is built up by applying a series of reinforcing layers and liquid resin layers. The curing process takes place at room temperature. Sandwich constructed composites can also be manufactured by this process.

It is relevant to refer that quality control in the hand lay-up process is difficult as it depends mostly on the operator skill, being one of the reasons inducing manufacturers to resort to other processes. Another disadvantage are the concerns about the styrene emission due to its open mould nature.

Spray-up

Spray-up process is an open mould method similar to the hand lay-up process in its suitability for making boats, tanks, transportation components, and tub/shower units in a large variety of shapes and sizes. A chopped laminate has good conformability and is sometimes faster to produce than a part made with hand lay-up when moulding complex shapes [5].

In the spray-up process, the operator controls thickness and consistency, which makes the process more operator dependent than hand lay-up. Although production volume per mould is low, it is feasible to produce substantial production quantities using multiple moulds and generating the possibility of automatizing the process. Spray-up uses simple, low cost tooling and it is of simple processing. Portable equipment grants on-site fabrication with virtually no part size limitations.

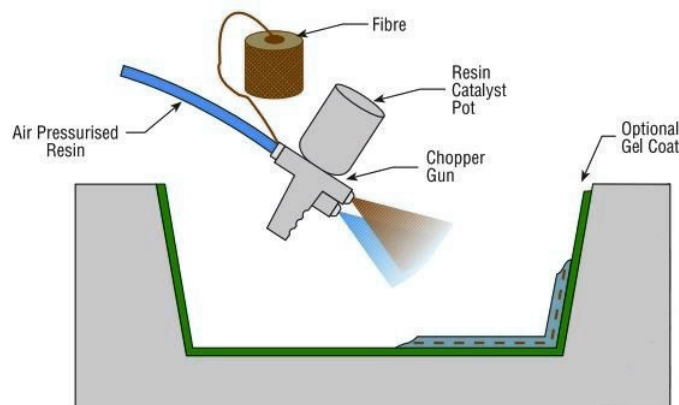


Figure 2.5: Schematic view of the spray lay-up process [3].

As in hand lay-up process, gel coat is first applied to the mould and allowed to cure. Continuous roving and resin are then fed through a chopper gun, which deposits the resin-saturated “chop” on the mould, as represented in Figure 2.5. The laminate is then rolled to thoroughly saturate and compact the chop. Additional layers can be added as required to obtain the designated thickness. Roll stock reinforcements, such as woven roving or knitted fabrics, can be used in conjunction with the chopped laminates and core materials can be easily incorporated [10].

Filament winding (FW)

Filament winding (FW) process, used for the manufacture of a wide variety of composite parts and components, has proved to be technically effective and cost competitive through the last few decades. Axis-symmetric composite parts like sewage or supply piping systems, high pressure vessels, aircraft fuselage sections, transmission shafts but also non axis-symmetric ones like wind turbine blades, buses chassis are among these identified applications [50].

The manufacturing process is depicted in Figure 2.6, it consists of an automated process in which an impregnated continuous filament (or tape) tow is wound over a rotating mandrel. The synchronized movement of both this mandrel and the delivery head in its moving carriage controls the fibre path, leading to the desired pattern (Figure 2.7).

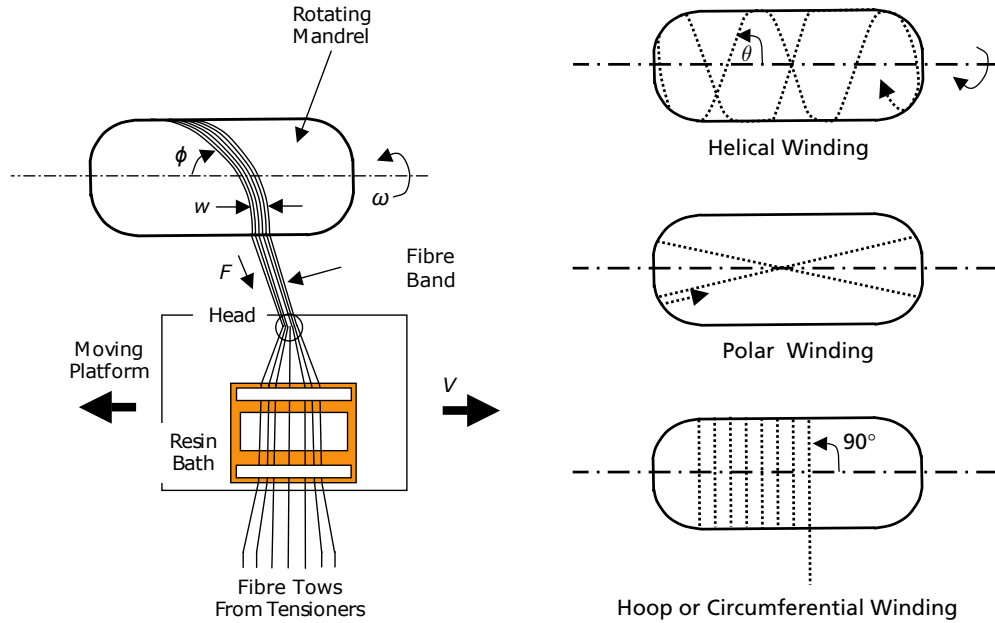


Figure 2.6: Schematic view of the FW process [2]. Figure 2.7: Filament winding patterns [2].

In FW, a computer numerical control (CNC) system allows the user to tailor a control package to his immediate needs while also facilitating expansion for future needs as required. Three computer controlled axes of motion provided on the traverse assembly, i.e., traverse (X-axis) motion, crossfeed (Z-axis) motion, and feedeye rotation enable winding of circumferential and helical patterns as well as conical shapes. Filament content in this process can be up to 80% so that high stiffness and strength, in the reinforcement direction, are possible [51].

This process is classified as being a very fast, and therefore economic, method of laying material, with a resin content that can be controlled by metering the resin onto each fibre tow through nips or dies. The fibre cost is minimised since there is no secondary process to convert fibre into fabric prior to used and the overall structural

properties of laminates can be very good, since it is possible to lay straight fibres in a complex pattern to match the applied loads. Nevertheless, the process is limited to complex geometrical parts, the external surface of the component is unmoulded, and therefore cosmetically unattractive, and low viscosity resins usually need to be used with their attendant lower mechanical properties [3].

Roll wrapping

In the roll-wrapping process, also called tube rolling, a prepreg sheet is first rolled out on a cutting table and cut to rectangular or trapezoidal shapes (either manually or with the help of an automatic prepreg cutter) with specific fibre orientations. It is then rolled around a mandrel, as illustrated in Figure 2.8. The outer diameter of the mandrel thus determines the inner diameter of the final tube. The mandrel and cloth are then spiral wrapped with a consolidation tape under tension to hold the laminate in place during the curing phase. After curing, the mandrel is extracted to leave the tube ready for machining or finishing as necessary [52, 53].

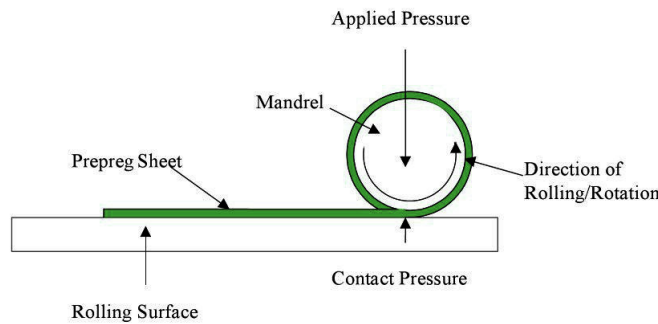


Figure 2.8: Schematic view of the roll wrapping process [4].

This process requires a low initial investment and is suitable for high-volume production of tubular components. It is mostly used to manufacture golf shafts, fishing rods, bicycle frames, and other tubular shapes [5].

2.2.3 Closed moulding processes

Closed mould processes are used to produce precision parts at lower costs for a variety of applications and are usually automated and used for high production volumes. In these processes, composite materials are processed and cured inside a vacuum bag or a two-sided mould, closed off from the atmosphere.

Compared to open moulding, closed moulding processes enable manufacturers to make better parts faster and more consistently, with less waste. Finished parts have better surface finish, reducing the need for post work. These processes are also less operator dependent and may require fewer moulds, reducing tooling costs [54, 10].

A subgroup of closed moulding processes worth mentioning is liquid composite moulding (LCM) processes. In LCM processes, a dry or partially impregnated fibrous preform is placed in a closed mould cavity and the empty spaces between the fibres are filled with resin by transferring the liquid resin from a reservoir under positive pressure or by drawing the resin into the mould by subjecting the mould to a vacuum. This family of processes came from the many variations of one process, the resin transfer moulding (RTM) process, which is described later in this chapter, and appeared during the decades of its development, while trying to overcome the challenges that were appearing.

The LCM processes, together with the vacuum bag only (VBO) process, also reviewed in this chapter, are categorised as Out-of-autoclave (OoA) processes [11].

Compression moulding

Compression moulding is one of the most common processing techniques to fabricate plastic and polymer composite products. It has been in use for a century and its usage has evolved greatly until today. It is a high-volume, high-pressure method suitable for moulding complex parts on a rapid cycle time and it can be used for processing of both thermosetting and thermoplastic materials.

There are several types of compression moulding, which are defined by the type of material moulded. The most common materials used are sheet moulding compound (SMC) and bulk moulding compound (BMC), although thick moulding compound (TMC) is also used. A compression moulding further use is in the making of structural panels in which prepregs and core materials are used.

The compression moulding process is composed of four basic phases: charge preparation and placement, mould closure, curing and part release (Figure 2.9).

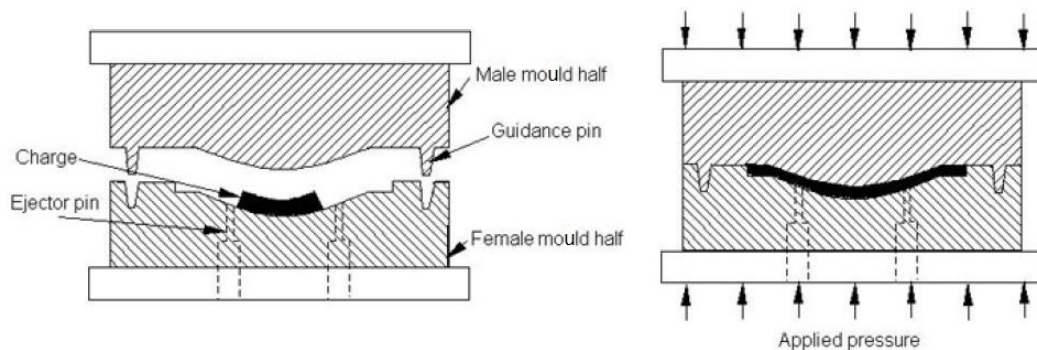


Figure 2.9: Schematic view of the Compression moulding [5].

The moulding compound is placed in an open and heated mould. The charge dimensions are selected to cover about half of the mould surface area and its weight is measured before its placement. The position of the charge in the mould is a key factor that affects the part quality since it influences the fibre orientation and void

content. A matched metal mould cavity is used to close the mould and continuous to move down slowly to compress the charge. The material flows to fill the mould and causes air to escape through the shear edges or air vents of the mould. The mould is then kept closed while the moulding pressure is maintained for a pre-assigned period of time, during which the resin is cured and the part consolidated. Finally, the part is removed from the mould with the aid of ejector pins and cooled down. Generally, the process cycle time ranges from 1 to 3 minutes depending on the part thickness [11].

Metallic moulds are used in this process and pressure is applied through a variety of methods including the tightening of screws, through press and other means to obtain high volume fraction of composites. Heat is also applied during the curing stage in some applications. Compression moulding enables part design flexibility and features such as inserts, ribs, bosses and attachments. It is possible to obtain good surface finishes, contributing to lower part finishing cost and minimizing trimming and machining operations and the labour costs are low [5, 48].

Injection moulding processes

Injection moulding is a commonly used polymer manufacturing process. Reaction injection moulding (RIM) and its two variants, reinforced reaction injection moulding (RRIM) and structural reaction injection moulding (SRIM) are more common in composite manufacturing. In this section all the above will be explained.

Injection moulding is one of the most important polymer processing methods for producing plastic and plastic composite parts. It is more common in the thermoplastics industry but has also been successfully used in the thermosets industry. It is a short fibre reinforced composite process and is capable of high production volume. It is characterised for having relatively low fibre volume fraction and good part finish. This process is suitable for consumer, automotive, and recreation applications. For the purpose of the present work, this description will be focused on injection moulding for thermoset composite parts.

The usual raw material for thermoset injection moulding is bulk moulding compound (BMC). It contains glass fibres, polyester resin, filler, additives, and pigment. For injection moulding, the fibre length is kept short, typically between 1 and 5 mm. Tool steel is used to make the moulds for injection moulding. Mould flow analysis is performed to come up with the right tool design. Tools for injection moulding are very expensive and complex, compared to other moulding processes (e.g., RTM). Injection moulding of glass fibre reinforced composites has the capability of producing near net shape articles having good physical and mechanical properties.

The process typically employs a reciprocating single-screw extrusion machine, as shown schematically in Figure 2.10. The machine is used for transporting, melting and pressurizing the fibre filled polymeric materials, which are fed into the machine in granular form. The polymer melts within the barrel by heat conduction through

the barrel wall and via the dissipation of heat generated within the sheared polymer melt. The melt accumulates in front of the screw, which is driven back against an adjustable pressure within the hydraulic system until a desired shot size (melt volume) is achieved. This is followed by injection where the screw pushes forward to force the polymer melt through a runner system and into the relatively cold empty cavity of the already closed mould. In order to compensate for any shrinkage caused by the cooling of the melt within the cavity, the melt in front of the screw is held under pressure so as to force more materials into the cavity. When the gate into the mould freezes, no more material can be supplied through the gate and the product cools down further without compensation for shrinkage. The mould temperature is regulated by water that circulates through channels to keep the mould cavity walls at a temperature between room temperature and the glass transition temperature (for amorphous polymers) or the melt temperature (for semi-crystalline polymers) of the polymeric materials. When the product is cooled to a state of sufficient rigidity, which in most cases occur when all regions of the part have cooled down to below glass transition temperature or melt temperature of the polymer, the mould opens and the product is ejected [11, 5].

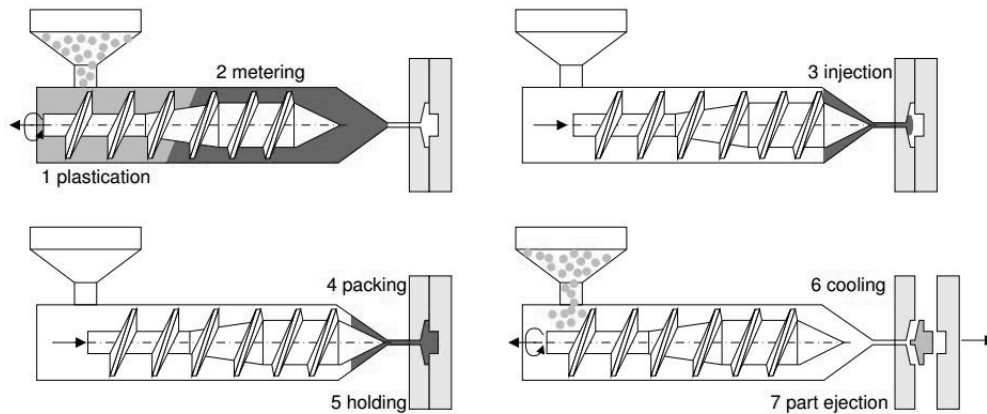


Figure 2.10: Injection moulding cyclic process [6].

Injection moulding is a cyclical process. Cycle times may range from 10 to 100 s and are controlled by the cooling time of the resin. It has the shortest process cycle time compared to any other moulding operation and thus has the highest production rate. The production rate can be further increased by having a multiple-cavity mould. Close tolerances on small intricate parts are possible with injection moulding. Typically, there is very little post-production work required because the parts usually have a very finished look upon ejection. All scrap may be reground to be reused to reduce the waste. Furthermore, full automation is also possible with injection moulding [11, 5].

Reaction injection moulding (RIM) takes its name from a chemical reaction that occurs within the tool. The plastics used are thermosets, either polyurethanes or foamed polyurethanes. The two components that produce the polyurethane are mixed just prior to injection into the tool, as represented in Figure 2.11. With the low viscosity and low injection pressures, large, complex parts can be produced eco-

nomically in low quantities.

Considerable design freedom is possible, including thick and thin wall sections (foamed polyurethanes are natural thermal and acoustic insulators). Excellent flow ability allows for the encapsulation of a variety of inserts.

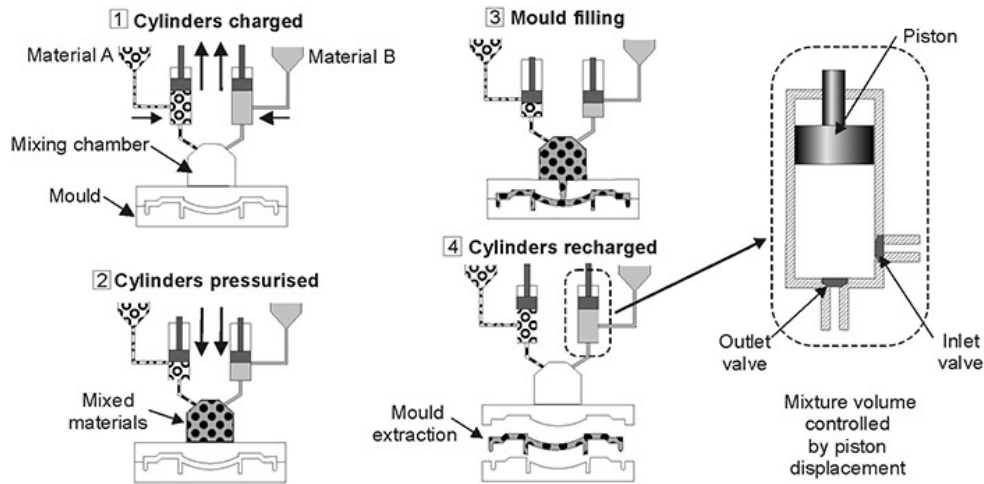


Figure 2.11: General steps of Reaction Injection Moulding (RIM) [7].

Reinforced reaction injection moulding (RRIM) uses reinforcements to improve the properties of the resin. With the use of reinforcements, polymerization shrinkage is reduced, thermal expansion is reduced, droop and sag of the composite at elevated temperatures is minimized and key properties such as stiffness, tensile strength and tensile elongation are improved. Milled fibres can be added directly to the resin before reacting in the mixing head. Metering is accomplished with high pressure pumps or injection cylinders. Typically, a small mixing chamber is used. The two resin streams enter from opposite sides of mix chamber under high pressure. Mixing occurs from the energy-intensive collision of these two resin streams. Although the streams are mixed at very high pressure, the result is a low viscosity liquid. The low viscosity mixed resin is easily injected into the mould at relatively low pressure. Polymerization takes place very quickly within the mould cavity with little or no additional heat required [10].

RRIM also as a variation of its own, the structural reaction injection moulding (SRIM) in which resin is injected to a mould cavity with chopped fibre preforms. The reacting resin remains liquid long enough to completely fill the mould and penetrate the reinforcing fibres, after which it quickly cures.

Injection moulding has several other less important variants such as in-mould surface decoration (ISD), hot-runner moulding (HRM) and gas-assisted injection moulding (GAM) [51], co-injection (sandwich) moulding and fluid-assisted injection molding [11].

Vacuum-assisted resin infusion (VARI)

Vacuum infusion resin infusion (VARI), also known simply as vacuum infusion (VI), can produce laminates with a uniform degree of consolidation, producing high strength, lightweight structures. This process uses the same low-cost tooling as open moulding processes and requires minimal equipment. Vacuum infusion offers substantial emissions reduction compared to either open moulding or wet lay-up vacuum bagging.

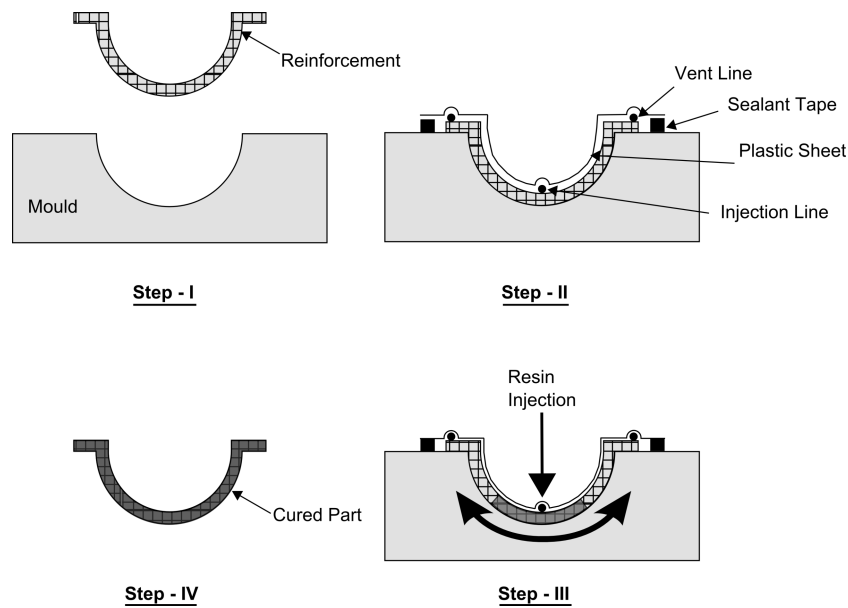


Figure 2.12: General steps of the Vacuum Infusion (VI) process [8].

Figure 2.12 shows the general steps of the VI process. First, reinforcement is laid on top of a rigid mould bottom half (Step-I). A sealant tape is laid around the periphery of the reinforcement, while injection and vent lines are positioned on top of it. The injection and vent lines pass through the sealant tape to connect to a resin source and a vacuum pump, respectively. Additionally, a resin trap can be added between the vent line and the vacuum pump to prevent resin from entering the vacuum pump and causing damage. Then, the mould is covered with a flexible vacuum bag. This vacuum bag attaches to the sealant tape to seal the mould and acts as the top half of the mould (Step-II). In addition, if required, the injection and vent lines can also be passed through the plastic sheet provided sufficient sealing is maintained. The vacuum pump evacuates air from inside the mould, thus creating a negative pressure gradient. This negative pressure gradient drives resin from its source through the injection line into the porous reinforcement (Step-III). Once the reinforcement is completely infused, resin injection is stopped while the vent is kept open and resin is allowed to cure before extracting the finished part (Step-IV).

Resin film infusion (RFI)

Resin film infusion (RFI) is a hybrid process in which a preform is placed in a mould on top of a layer or interleaved with layers of high-viscosity resin film. It has been developed as a cost effective replacement for autoclave process.

In RFI, dry fabrics are laid-up interleaved with layers of resin film supplied on a release paper. The lay-up is vacuum bagged to remove air through the dry fabrics and then heated in an oven to allow the resin to first melt and flow into the air-free fabrics, and then after a certain time, to cure. The lay-up is depicted in Figure 2.13. The result is a uniform resin distribution (even with high-viscosity, toughened resins, because of the short flow distance) and high fibre volumes with low void contents [9, 55].

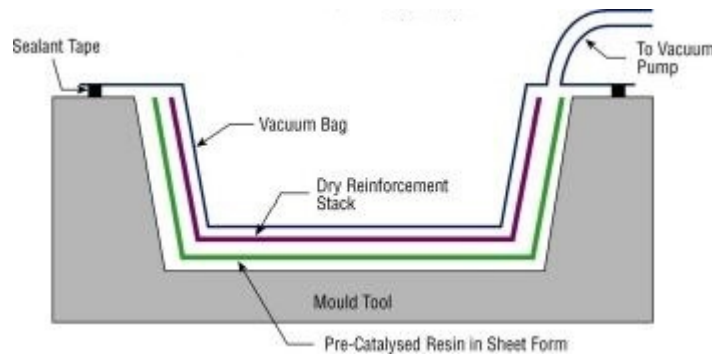


Figure 2.13: Schematic view of the resin film infusion process [9].

The resin film needs to be stored at -18°C , similar to prepreg materials; however, since sandwiching can be done on demand, only resin films need to be stored at lower temperatures, thus exceeding shelf life results in the loss of only resin films. Furthermore, RFI produced parts have excellent structural properties, excellent drapability and a very low void content.

Centrifugal casting

In centrifugal casting, reinforcements and resin are deposited against the inside surface of a rotating mould. Centrifugal force holds the materials in place until the part is cured.

The reinforcement, roving or, for small diameters, fabrics, mats or complexes and resin, are introduced into a rotating, cylindrical, metal mould as depicted in Figure 2.14. The resin impregnates the reinforcement under the effect of the centrifugal force and forms, after polymerization, a cylindrical structure. The speed of rotation is increased until the moulding speed is reached, which depends on several factors, such as, the amount and nature of the reinforcement, the thickness and diameter of the part and the viscosity of the resin.

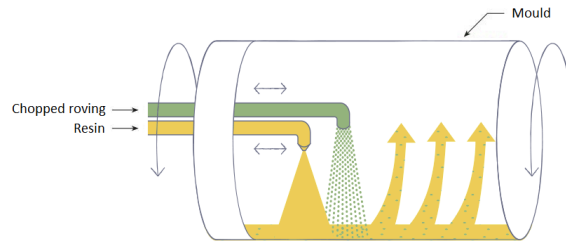


Figure 2.14: Schematic view of the Centrifugal Casting process [10].

This process is suitable for the production of hollow parts, such as pipes, with two smooth surfaces. The outside surface of the part, which is cured against the inside surface of the mould, is the finished surface. The interior surface can be given an additional coating of pure resin to improve surface appearance and provide additional chemical resistance in the part. It is particularly well suited for producing structures with large diameters: pipes for oil and chemical industry installations, water supply, tanks for the storage of wine, milk or chemical products. It is being increasingly used to produce poles, such as telephone and street lighting poles. Moreover, centrifugal casting contains volatiles during processing and its productivity per tool is relatively low [10, 56].

Continuous lamination

Continuous lamination is a highly automated process which makes composites in sheet form such as composite glazing, corrugated or flat construction panels, and electrical insulating materials.

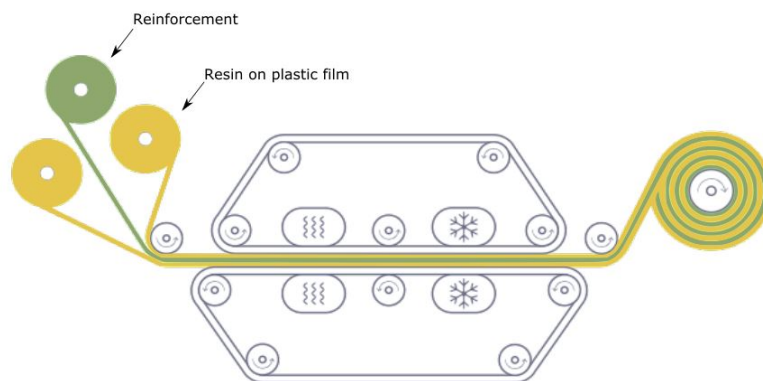


Figure 2.15: Schematic view of continuous lamination [10].

As outlined in Figure 2.15, the reinforcement fibres are impregnated with resin and sandwiched between two plastic films. The sheet takes shape under forming rollers and is then guided through pressing and guiding rolls so the desired composite lay-up is formed. Typically, high output machines up to 3 meters wide are used in the continuous lamination process. As the material is passed through a

heating zone, the resin is cured to form the composite panel. The structure consists of several reinforcement layers depending on strength, stiffness and other required properties.

Panels are automatically trimmed to width and cut to length. Corrugated sheet is produced by forming shoes which hold the compacted sheet in the required shape during cure and special surface effects are created by using embossed carrier films that are later removed. Both mat reinforcements and rovings chopped by special wide cutters are employed in the process. Polyester and acrylic modified polyesters (for improved water resistance) are the primary resins for continuous lamination [57, 54, 10].

Pultrusion

Pultrusion is a continuous process for manufacturing composites with constant cross-sections or structural profiles having significantly long length. It is widely employed in the composites industry due to its continuous, automated and highly productive nature.

Raw materials are a liquid resin mixture (containing resin, fillers and specialized additives) and flexible textile reinforcing fibres [58].

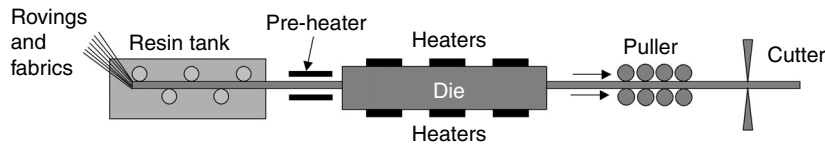


Figure 2.16: Schematic view of the pultrusion process [11].

While pultrusion machine design varies with part geometry, the traditional pultrusion process concept is described in the schematic shown in Figure 2.16. As depicted in the figure, the pultrusion process starts with the pulling of reinforcing fibres in the forms of continuous rovings or mats from a series of creels. The fibrous material is fed continuously through a guiding system into a resin bath to get it impregnated. The resin-soaked fibres are guided to a heater assembly to preheat the fibre-resin mix while shaping it close to the desired finished profile. The same is then taken into a heated die where curing of thermosetting resin is initiated by the heat. The cured part subsequently leaves the die in the desired shape where it is cut into the required lengths using a cut-off saw without interrupting the continuous pultrusion process.

Some disadvantages exist in the traditional thermosetting and thermoplastic pultrusion processes and so studies have been conducted in various key features and problem areas. These have resulted in a number of pultrusion variants that combine conventional pultrusion and other processes, such as compression moulding and injection moulding processes, have gained attention due to the ability to integrate the

best qualities of different basic processes.

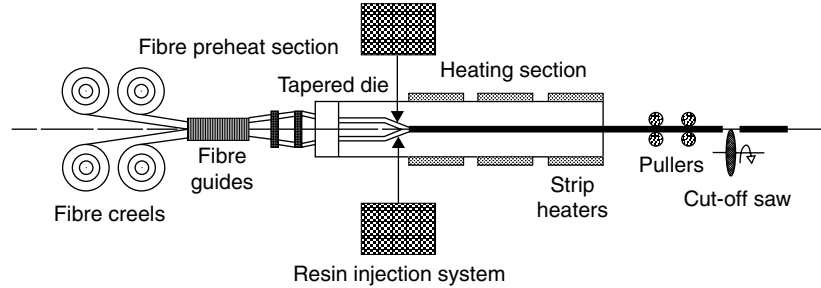


Figure 2.17: Schematic view of injected pultrusion [11].

Injected pultrusion (IP) is a hybrid technique of traditional pultrusion and resin transfer moulding (RTM). The process is similar to RTM in that the thermoset resin is injected through the top and/or bottom injection gates into the dry reinforcement after it is pulled into the injection-pultrusion die (Figure 2.17). The rest of the process is similar to traditional pultrusion. This process not only allows a higher pull speed but also significantly reduces the volatile emissions due to the elimination of the open resin bath in the process [11].

QuickstepTM process

The QuickstepTM process technique was developed by Quickstep Technologies Pty Ltd and was patented in 1996. Figure 2.18 highlights the principles involved in the Quickstep process.

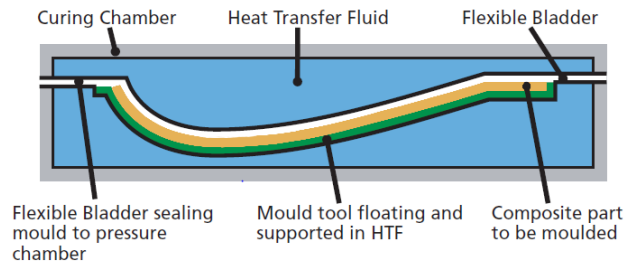


Figure 2.18: Schematic view of QuickstepTM process [12].

QuickstepTM is a balanced pressure, heated mould process that can be utilized for curing of advanced composite materials. The process uses an unique fluid-based technology for curing the composite materials. It works by rapidly transferring heat to and from the laminate positioned between two free floating rigid or semi-rigid moulds that float in a Heat Transfer Fluid (HTF). As fluids have a much greater volumetric heat energy capacity than gases, the heat transfer rate between the fluid and laminate is much higher than that achievable in an autoclave or other oven. The mould and laminate are separated from the circulating HTF by a flexible membrane or bladder. The high heat capacity and thermal conductivity of the heat transfer

fluid allows a fast and efficient cure. The HTF can be rapidly heated and then cooled to cure the laminate allowing excellent consolidation to be obtained at low application pressures. Due to high heating and cooling rates during the processing of composites, the reaction exotherms are not manifest as a significant temperature rise within the lay-up, because the circulating fluid removed any excess heat generated, during the process. Meaning that a constant cure temperature may more easily be maintained, even for thick laminates. Further benefits of the process include the fact that low pressure processing allows for the use of lighter weight cores and that the process benefits from versatile production facilities, reduced capital, tooling and operational costs [48].

QuickstepTM's highly flexible manufacturing route through high-rate production principles is expected to allow composites manufacturers to move away from a batch manufacturing philosophy, where a large number of uncured parts are installed in the processing plant and cured together, to a more flexible, one-piece flow where individual parts are prepared and cured in an assembly line process.

Although this process offers many potential benefits it is not yet used in serial production. Therefore, a lot of questions related to stability and reliability cannot be answered. It can be expected that the lifetime of a flexible membrane is limited and replacement could take time. It is also possible that the flexible membrane, when aged, will fail during a cure cycle, which could potentially compromise the parts being cured [11].

Resin transfer moulding (RTM)

Resin transfer moulding (RTM) is an intermediate volume moulding process for producing composites [10]. This process was adopted for composite manufacturing in the mid-1980s having a driving force in the automotive industries. This could be done by injection and compression moulding of discontinuous fibres but the structural performance could not be achieved by short fibres. In contrast to these moulding processes, the RTM process offers production of cost-effective structural parts in medium-volume quantities using low-cost tooling. Complex parts with controlled fibre directions can be manufactured. Continuous fibres are used in the RTM process. Only low viscosity resins were possible candidates due to the resistance to flow because of the micro level empty spaces between the fibres. Thus, the resins of choice for this process are thermosets, although there has been some more recent activity in bringing to market thermoplastic resins with low viscosity.

As illustrated in the schematic of Figure 2.19, the RTM mould has a cavity in the shape of the part to be manufactured. A preform is placed on the tool surface of the mould, usually machined from tool steel which allows long lives for large production runs and is resistant to handling damage. Once the fibre plies are placed and the edges trimmed, a matching mould half is mated to the first half and the two are closed and clamped together, resulting in the compaction of the preform to the specified fibre volume fraction. Clamping can be accomplished with perimeter clamping or press clamping. The mould is heated to a specified temperature. The

resin is then injected under pressure (0.1-2 MPa) and at a selected temperature, using mix/meter injection equipment, into the cavity through one or more gates under positive pressure positioned in strategic places. Sometimes, a vacuum is created inside the mould to assist in resin flow as well as to remove air bubbles. The resin injection is continued until it is completely filled and the resin is seen exiting from the vent ports. At this point, the resin injection is discontinued, vent ports are closed and the pressure inside the mould is increased to ensure that the remaining porosity is collapsed. The resin is allowed to cure. Curing takes 6 to 30 minutes, depending on the cure kinetics of the mixture. After the part has hardened, the mould is opened and the part is demoulded. The cure may be initiated by heating the mould, although for large tools the heat-up rates will be extremely slow, and/or by addition of inhibitors to the resin system initially. Heated moulds are required to achieve fast cycle times and product consistency. RTM parts are frequently given free-standing post-cures in ovens after demoulding [11, 5, 2].

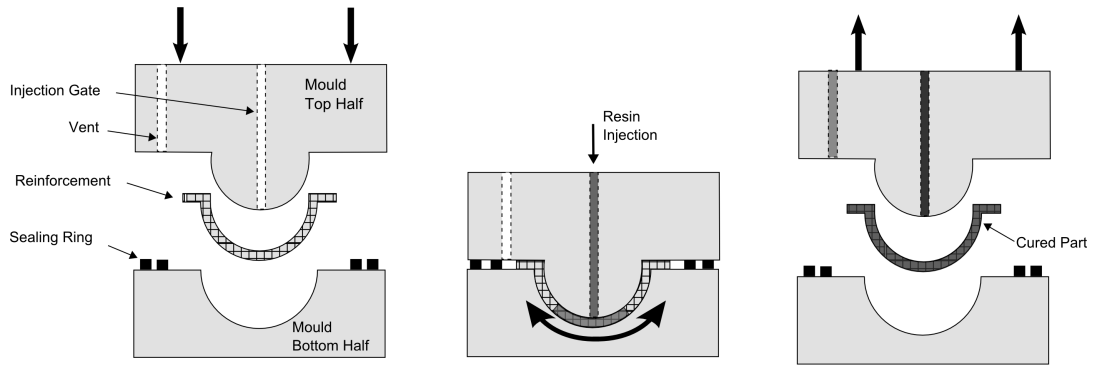


Figure 2.19: Schematic view of RTM [8].

By laying up reinforcement material dry inside the mould, any combination of materials and orientation can be used, including 3D reinforcements. Part thickness is determined by the tool cavity. Fast cycle times can be achieved in temperature-controlled tooling and the process can range from simple to highly automated.

RTM can use a wide variety of tooling, ranging from low-cost composite moulds to temperature controlled metal tooling. Due to the high injection pressures and often high temperatures involved, RTM tools are bulky and costly to manufacture and to process. Steel-matched metal moulds have two major disadvantages, being expensive, and having slow heat-up and cool-down rates. Matched metal moulds have also been fabricated from Invar 42 to match the coefficient of thermal expansion of carbon composites, and from aluminum because it is easier to machine (being less costly) and has a high coefficient of thermal expansion which can be useful in some applications, but is much more prone to wear and damage than steel or Invar. For prototype and short production runs, matched moulds can be made of high temperature resins that are frequently reinforced with glass or carbon fibres. RTM tooling returns parts with two finished surfaces.

The preform used in the RTM process should be designed by selecting adequate fibre and fabric types and fibre volume fraction considering the mechanical performance, permeability to resin flow, fibre wet out, formability and cost.

The RTM process has several variations, one of the most important being the vacuum assisted resin transfer moulding (VARTM). This is very cost-effective process in making large structures such as boat hulls. A typical VARTM process, shown in Figure 2.20, consists of single-sided tooling with a vacuum bag. VARTM processes normally use some type of porous media on top of the preform to facilitate resin distribution. The resin is drawn into the mold from a reservoir at atmospheric pressure. The porous distribution media should be a highly permeable material that allows resin to flow through the material with ease. When a distribution media is used, the resin typically flows through it and then migrates down into the preform. Typical distribution media include polyamide (PA) screens and knitted polypropylene. Since resin infiltration is in the through-the-thickness direction, race tracking and resin leakage around the preform are largely eliminated.

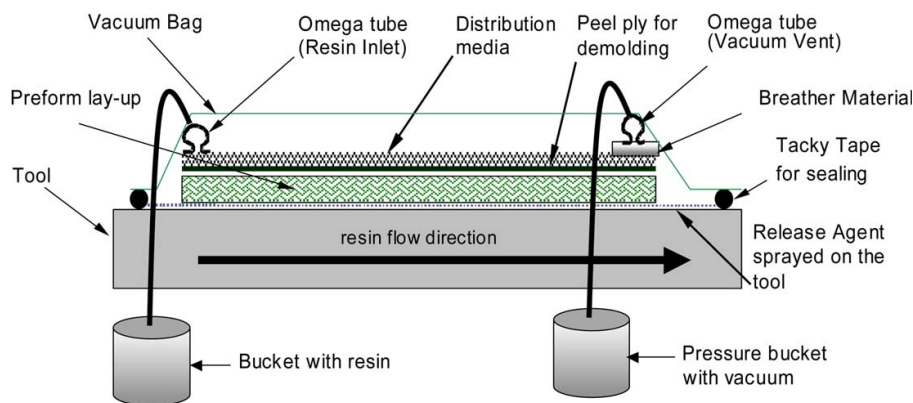


Figure 2.20: Schematic view of VARTM process [13].

As the VARTM process uses only vacuum pressure for both injection and cure, autoclaves are not required and very large part sizes can be made. Ovens and integrally heated tools are normally used, and since the pressures are low, low-cost lightweight tools can be used. A layer of breather between the two bags increases the ability to remove any air from leak locations. The resins used for VARTM processing should have even a lower viscosity than those used for traditional RTM so that the flow is able to impregnate the preform at vacuum pressure. Vacuum degassing prior to infusion is normally used to help remove entrained air from the mixing operation. The resin source and vacuum trap should be kept away from the heated tool so that the temperature of the resin at the source is easier to control and the chance of an exotherm at the trap is minimized.

In VARTM, the pressure is much lower than that normally used in the conventional RTM or autoclave processes and it is more difficult to obtain as high a fiber volume fraction as with the higher pressure processes, although, this disadvantage is being overcome with near net preforms. Another disadvantage is the filling

being very slow, as only one atmosphere is available for resin infusion. In addition, as the top surface is flexible, resin pressure as it flows into the mold will change the compaction and hence the fibre volume fraction during impregnation resulting in non-uniform fibre volume fraction in the part unless certain steps are taken to prevent it. Furthermore, the VARTM processes cannot hold as tight dimensional tolerances as conventional RTM, and the bag side surface finish will not be as good as a hard tooled surface. Thickness control is generally a function of the perform lay-up, the number of plies, the fibre volume fraction and the amount of vacuum applied during the process [2, 59].

A variation of the VARTM process is SCRIMP, Seemann Composite Resin Infusion Moulding Process. In this process, a steady vacuum is drawn to first compact the layers and then to draw resin into the layers. In this way, fibre compaction occurs before the filaments and core are infused with resin, thus eliminating voids and ensuring accurate placement.

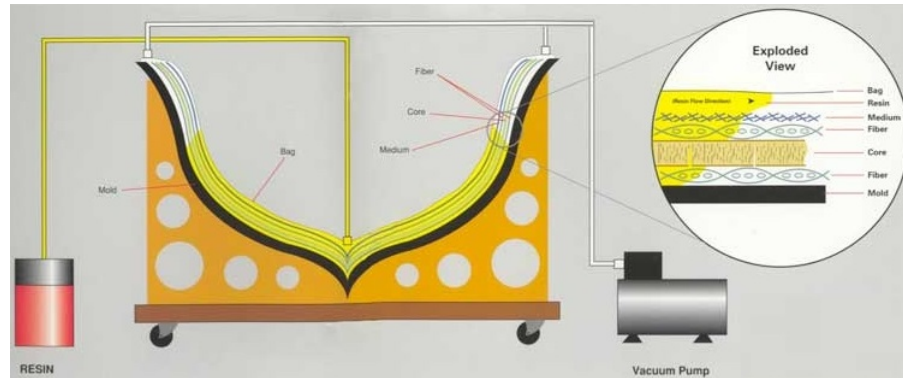


Figure 2.21: Schematic view of SCRIMP [14].

SCRIMP overcomes one of the major disadvantage of VARTM, the slow filling due to the limited pressure differential between the inlet and exit which cannot exceed one atmospheric pressure. This is accomplished by adding a peel-ply and a distribution medium of much higher porosity (and thus higher permeability) than the fibre preform and placing it between the preform and the vacuum bag as shown in the schematic in Figure 2.21. Resin initially races through the distribution medium due to its high permeability in the in-plane directions and then it needs to penetrate only across the thickness direction which is a very short path compared to in-plane directions. The design of the distribution medium, i.e., its size and location in the mould, must be carefully crafted to ensure complete mould filling, otherwise the resin could reach the vent before saturating the preform completely. As compared to RTM, the issue of gradient in the fibre volume fraction still remains due to the absence of a rigid top mold to prevent the preform from expanding as the resin enters the preform relieving some of the atmospheric pressure being applied on the flexible bag.

The major use of the SCRIMP process is in the marine industry as it works especially well for medium to large-sized parts. Applications for the SCRIMP pro-

cess include marine docking fenders for seaports, windmill blades, satellite dishes, railroad cars, buses, amusement park rides and aerospace components [5, 11].

High pressure resin transfer moulding (HPRTM) is another variation of RTM relevant to describe. In this process, the equipment technology allows injection of resin under high flow rate in the mould cavity. The equipment used contains high-pressure pumps for dosing resin and hardener and a self-cleaning mixing head, this combination guarantees precise resin and hardener mixing along with materials injection into the mould at constant defined flow rate (0.02-0.2 kg/s) though high flow resistance is created in the mould cavity. HPRTM has two different variants, high-pressure injection RTM (HPIRTM) and high-pressure compression RTM (HPCRTM).

The HPIRTM process differs from the classical RTM process only in terms of the processing equipment for the resin system. The resin injection sequence of the HPIRTM process is shown in Figure 2.22. In the classical RTM process, lower pressure mixing and dosing equipment is used for processing the resin, whereas in the HPIRTM process resin mixing and dosing is carried out using high-pressure equipment. The resin and hardener mixture is injected into the cavity under high injection speed, which allows the cavity to fill quickly, significantly reducing the resin injection time. For this reason, this process variant allows the use of resins with relatively high reactivity [15].

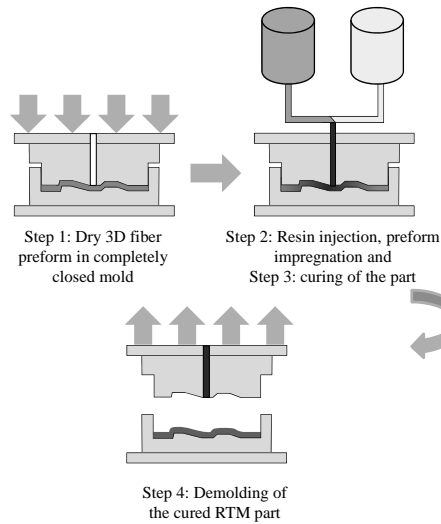


Figure 2.22: Resin injection sequence in the HPIRTM process [15].

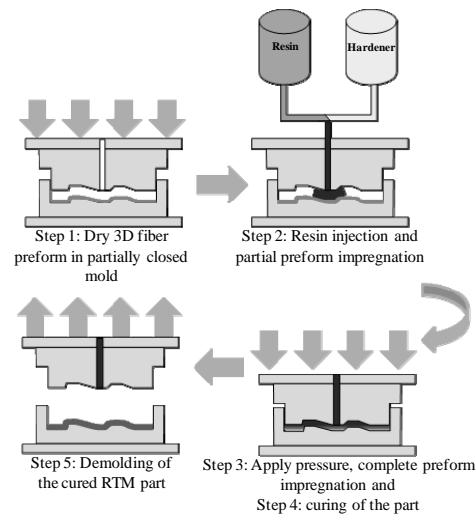


Figure 2.23: Resin injection sequence in the HPCRTM process [15].

As depicted in Figure 2.23 the HPCRTM process is a combination of RTM and compression molding. Similar to the HPIRTM process, high pressure RTM equipment is used for processing of resins. If conducted without the use of high pressure RTM equipment, the process is referred to in the literature as the compression resin transfer moulding (CRTM) process. In HPCRTM, the preform is placed into the mould cavity and it is closed partially, leaving a small gap between the upper mould

surface and the fibre preform. The resin is introduced into the gap and flows easily over the preform and may partially impregnate it. Once the required amount of resin has been injected into the gap and the injection point is closed, the mould closes further and applies high compression pressure to impregnate the resin into the preform, especially in the through thickness direction. The preform is compacted to achieve the desired part thickness and fibre volume fraction. The part can be demolded after the resin has cured. The quick resin injection and fast impregnation by applying compression force allows this process to be used for highly reactive resins, allowing faster manufacturing of the high-performance composites [15].

Other variants of the RTM process include light resin transfer moulding (LRTM) and closed cavity bag moulding (CCBM), also referred to as reusable bag moulding, which combines the benefits of LRTM and VI, among others.

Vacuum bag only (VBO)

A new generation of out-of-autoclave (OoA) preregs has been introduced not long ago, and experience with these preregs has demonstrated that it is possible to produce autoclave-quality parts using VBO consolidation. VBO preregs, which encompass traditional hand lay-up as well as automated material placement methods, are of particular interest due to a combination of unique advantages [60]. By avoiding the use of autoclaves, such materials significantly reduce acquisition and operating costs and are compatible with a diverse range of lower-cost cure set-ups, including conventional ovens, heating blankets, and heated tooling. In addition, the lower cure pressure supplied during VBO cure can eliminate autoclave-induced defects such as honeycomb core crush, allowing the use of lighter (and less expensive) cores [16].

OoA preregs have recently been developed and considered for the manufacture of high quality parts under limited VBO consolidation pressure. The particularity of these preregs comes from their internal microstructure: the fibre bed is partially impregnated with resin, consisting of both dry and resin-rich areas, as visible in Figure 2.24. Consequently, VBO preregs are often referred to as semi-impregnated preregs, or semi-preregs [61].

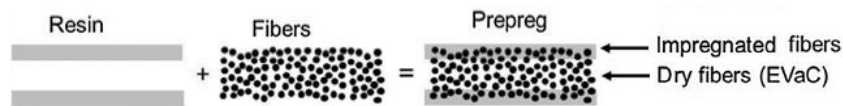


Figure 2.24: Schematic and micrograph of air evacuation channels in VBO prepreg [16].

By controlling the resin impregnation process, material suppliers offer semi-preregs featuring dry fibre tow regions, which makes them "breathable", acting as denoted as "engineered vacuum channels" or "EVaCs". As a result, application of vacuum allows entrapped gases in the laminate stack to escape through the dry regions and towards the laminate boundaries in early processing (Figure 2.25). Then, at elevated temperature, the resin flows and infiltrates the dry fibres, producing

laminates with less than 1% porosity [61].

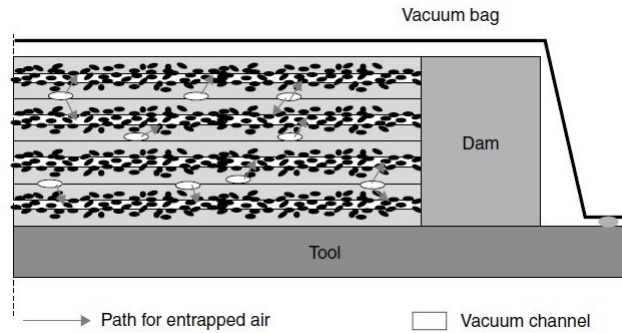


Figure 2.25: Schematic of evacuation of entrapped air from VBO prepreg. [11].

A common VBO lay-up, with appropriate consumables identified, is presented in Figure 2.26.

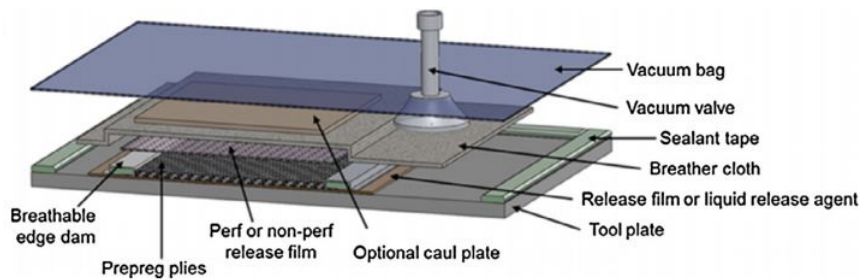


Figure 2.26: VBO lay-up schematic [16].

The part design, materials, and manufacturing equipment are first selected. The tooling is then cleaned and a mould release agent is applied. VBO prepreg plies and consumables are hand-cut to the required size and shape. The consumables consist of tool-side non-perforated release film, bag-side perforated release film and breather, perimeter edge breathing dams made of sealant tape wrapped in fibre-glass boat cloth, and a vacuum bag. The prepreg plies are manually stacked on the tool to form the laminate, with or without intermediate de-bulking, and the bag is assembled, sealed, and leak tested. Then, a cure cycle is selected based on the chosen prepreg resin and cure set-up. Curing consists of a room-temperature vacuum hold to evacuate entrapped air, followed by one or more high-temperature ramps and dwells. The only source of pressure applied to the stack of prepreg plies is the difference between the atmospheric pressure and the bag pressure (vacuum), significantly reduced compared to conventional pressurized autoclaves. Vacuum is drawn using a standalone, dedicated vacuum pump, while heat is imparted using a convection oven or other non autoclave set-up. An instrumentation system (consisting of a computer, a digital acquisition system, and temperature sensors) is used for basic process monitoring. No human activities are associated with the room temperature hold or cure, other than placing and removing the part from the oven, and de-bagging. Finally, post-machining is carried out on the manufactured part: most

typically, the edges are trimmed to a predetermined depth to remove resin flash [62].

Design, material, and equipment selections govern the part size and lay-up (amount of material) as well as direct material and equipment costs. Prior to cure, the material use efficiency is affected by prepreg and consumable cutting, which can generate waste as plies are extracted from roll stock. Moreover, the duration and efficiency of human activities influence labour costs. The length of the cure cycle is governed by the cure kinetics of the resin at a given dwell temperature and the heat-up and cooldown ramp rates achievable by the cure set-up. In addition, energy consumption during cure directly influences operating costs. Finally, post-machining can generate further waste [62].

2.3 Curing process

The term “plastic” is used to describe the moulded form of a synthetic resin. These resins are composed of large, chain-like molecules known as polymers, which also occur naturally as, for example, cellulose, protein and rubber. Most synthetic resins are made from chemicals derived from oil and it is these artificial polymers which are used to produce what are commonly known as “plastics”. Curing is a term in polymer chemistry and process engineering that refers to the toughening or hardening of a polymer material by cross-linking of polymer chains. This is achieved either by the use of a catalyst and heating, or at room temperature by using a catalyst and an accelerator [63].

In autoclave processing, prepregs, thin layers of high modulus fibre impregnated with partially cured resin, are used. The resin is cured after assembly in the autoclave where pressure and temperature are applied to the laminate according to a predetermined cure cycle. The resin polymerization reaction is triggered by the heat of the autoclave. The heat transfer medium in this process is usually compressed nitrogen [11].

In oven processes, the heat transfer is based on the same principle as the autoclave: convection heating. Although the heat transfer medium is normally air, different from the compressed nitrogen common in the autoclave. The specific heat capacity of air is lower than compressed nitrogen which makes it slower to react. This means that the effect and risk of exothermic reaction can only be restricted by ramping up the temperature very slowly and with very accurate control [11].

In RTM, after preforms, thin layer of high modulus fibre, are laid-up and the mould is closed, the resin is injected into the mould cavity through one or more gates under positive pressure, either under constant flow rate, or constant pressure. After complete mould filling, the cross-linking of the thermoset polymer is usually achieved at elevated temperatures. The cure may be initiated by heating the mould and/or by addition of inhibitors to the resin system initially [11].

In VBO, semipregs, thin layers of high modulus fibre semi-impregnated with partially cured resin, are used, ensuring even resin distribution and avoiding the dry

spots and resin-rich pockets, common with infusion processes. These prepregs can be cured at lower pressures and temperatures than the ones used in autoclave processing (atmospheric pressure and cure at approximately 120°C compared to 700–1000 kPa and 180°C autoclave cure). Nevertheless, after curing a part at 120°C, a free-standing post-cure at elevated temperature (usually, 180°C) is recommended to achieve a final higher T_g (glass transition temperature) and improved mechanical performance [11].

2.4 Manufacturing defects

This section has the purpose of describing the most common processing defects in composite materials, particularly when manufactured by the three processes in study.

The effect of the processing parameters towards the manufacturing defects can be divided in its sub-processes. Which are, for autoclave and VBO, lay-up, vacuum bagging and curing, and for RTM lay-up, injection and curing.

One of the major defects which may occur during the manufacturing of fibre reinforced composites is the creation of voids which are known to induce a severe degradation of mechanical performances [64]. To better understand void formation and its causes, several studies have been made over the years with the ultimate goal of predicting and learning how to avoid them.

In the autoclave process, voids can be formed due to an elevated number of reasons, such as the entrapment of air in resin rich areas during the formulation of prepreg materials, the moisture absorbed during the storing, volatile resin components during the processing, inadequate values of temperature and pressure during the curing and tearing in the vacuum bag during a cure cycle. Many studies have been performed to restrain the void formation and proper cure parameters such as pressure, duration or temperature were found, to reduce the appearance of voids. Nowadays, autoclave manufactured parts have a very low percentage of voids. Which is one of the reasons that makes replacing it such a difficult task.

The high pressures of the autoclave are the premier factor for the decrease in void formation, the relationship between void content and cure pressure was found to be an exponential decrease. The time frame of pressure appliance is also important, as the curing cycle can be optimized by applying pressure within the range of minimum viscosity. Moreover, the pressure in the autoclave reduces the size and geometry of the voids that do remain, they appear spherical and small at high pressures and larger and elongated as the pressure goes down [65]. The autoclave pressure is also sufficient to maintain the part void free in the presence of moisture [66].

There are many sources to create voids in composite manufacturing, but the previous studies have found that the mechanical air entrapment induced by the non-uniform flow is the main reason for the void formation in RTM. A dual-scale void content can be defined and characterized measuring the intra-tows micro-voids and the inter-tows macro-voids. This dual porosity leads to an impregnation mechanism

that is a consequence of a double scale flow. The resin can easily flow in open channels between the tows with less viscous resistance than in the inter-tows because of the differences in the local porosity. When viscous forces are dominant, i.e. for high resin velocity, micro-voids appear inside the fibre tows due to the difference between the viscous resistance of the tows and the open channels. In the opposite case, if capillary forces dominate the fluid flow, i.e. for low resin velocity, the impregnation is faster inside the tows than in the channels and macro-voids are formed between the tows in the open channels. The velocity difference between the two types of resin flow may result in the air entrapment. If the global resin velocity is large, the resin flows firstly in the macro-voids and entraps air in the micro-voids. On the contrary, void is created in the macro-voids if the global velocity is small and the capillary wicking inside tows leads the viscous resin flow through the macro-voids, as shown in Figure 2.27.

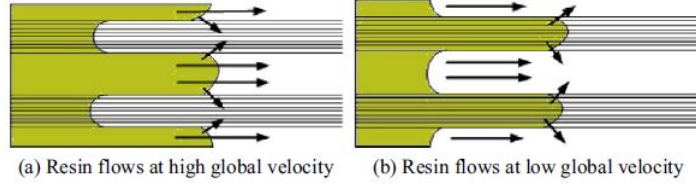


Figure 2.27: Void formation mechanism in the RTM process [17].

Relating to this, an important study has been made which is opportune to refer. It has been found that the formation of voids can be correlated with a dimensionless number called modified capillary number Ca^* which is a ratio of viscous force and surface tension,

$$Ca^* = \frac{\mu \bar{u}}{\gamma \cos \theta} \quad (2.1)$$

where μ is the resin dynamic viscosity, \bar{u} is the global resin velocity, γ is the surface tension of resin and θ is the contact angle between the resin and fibres. At low Ca^* macro-voids are formed and at high Ca^* , micro-voids appear. Therefore, a process window can be found around the optimal modified capillary number as shown in Figure 2.28, which has been used to optimize the resin injection flow rate [67, 17].

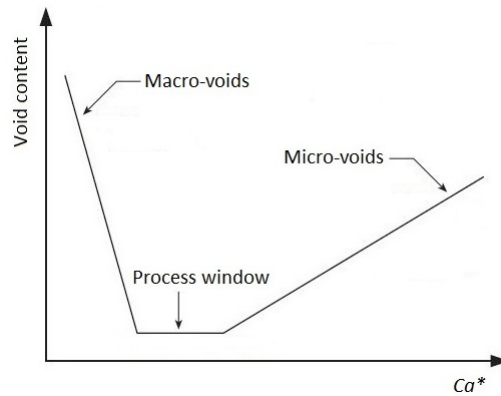


Figure 2.28: Void content as a function of modified capillary number [17].

Amongst other manufacturing induced defects, distortion in the fibres in the form of waviness, become significant when loaded in compression. Also associated with any disorientation in the fibre tow path is the accumulation of resin rich pockets. It was found that the presence of fibre waviness caused a significant reduction in the compression strength and that the failure initiated where the fibre misalignment was the greatest. In the case of resin rich regions the failure did not initiate from the resin rich layer itself, instead the initiation of delamination was found to occur at a region demarking the deformed and the undeformed layers [68].

In VBO, the semipregs themselves evolved with the realization that the key to the production of void-free parts using vacuum bag only methods is, counterintuitively, the introduction of open-cell porosity into the prepreg itself, through partial impregnation [16]. This knowledge reduced greatly the voids in VBO manufactured composite parts and made the process competitive in high performance composite materials industry. During processing, sources of porosity can be classified in two categories: flow-induced and gas-induced. Flow-induced porosity refers to a dry-fibre region left in a cured laminate due to the inability of resin to fully impregnate the dry areas before gelation. This type of defect is typically found in resin transfer processes, and is either caused by premature resin gelation, excessive resin loss or inadequate resin flow rates [61]. Under VBO consolidation, if material and thermal conditions combine to alter the resin viscosity too far from the designed range, partial impregnation makes VBO preregs susceptible to significant and potentially disastrous flow-induced micro-voids. These conditions include excessive out-time (or intermediate out-times and low-temperature cure) and form an intrinsic process limit for such materials. Flow-induced voids are purely a function of fibre bed and resin properties, and can occur regardless of how well gas-induced void sources are controlled. In the second category, presence of bubbles in the resin is caused by three distinct gas-induced mechanisms: air entrapment, cure-generated volatiles and vaporised moisture. In the absence of an elevated pressure safeguard, VBO preregs are vulnerable to any process deviation that reduces their void-suppression capacity, either through decreased resin pressure (from reduced ambient pressure) or, more likely, through increased void pressure caused by inadequate vacuum, insufficient air evacuation, or moisture vaporization. This sensitivity, in turn, motivates the need for strict material storage, handling and cure protocols [16].

Qualitative representations of the influence of various process parameters on void content are presented in Figure 2.29.

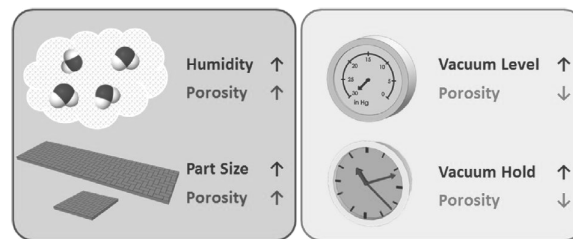


Figure 2.29: Influence of various process parameters on porosity in VBO composites [16].

Another common and greatly investigated prevailing defect in the manufacture

of composite parts is warpage. The curing warpage deformation refers to the certain degree of inconsistency between the ideal shape and the unexpected shape in the room temperature. In industries like aerospace, which require matching of smaller subcomponents in the assembly phase, poor dimensional fidelity of sub-components leads to increased assembly time and cost. One of the main reasons for this to happen is residual stress build-up during cure, resulting in warpage when the composite part is fully cured and removed from the tool. The expected warpage of the composite part is typically compensated for in tool design using past experience, i.e., is "added" to the tool geometry such that the warped part has the desired geometry, and although the concept of tool compensation is straight-forward in principle, each new part typically differs from previous parts in terms of either part and tool materials, geometry or lay-up, making it difficult to extrapolate past experience to new parts.

There are a number of mechanisms causing residual stresses and distortions, including differential thermal expansion, cure shrinkage and tool-part interaction. These operate throughout the cure cycle, with the importance of the effects varying as the resin passes through the two critical stages of gelation and vitrification. The main driving forces behind residual stress build-up are anisotropic thermal expansion and resin cure shrinkage.

In terms of the fabrication processing, there are a few solutions commonly used to manufacture a complex part. Integrated structures (the use of moulding technology in the design and manufacture to replace the parts connected to form the integrated structures) are generally divided into the following three ways: co-cure, co-bonding and secondary bonding. Different coefficients of thermal expansion (CTE) between composite materials are another source of process-induced deformation.

Simple formulas that predict the warpage of curved composite laminates are available in the literature and analytical and numerical models have been developed to predict the residual stresses in cured composite parts. However, there are many more factors that affect the residual stress build-up and subsequent warpage yet to be studied [69, 70, 71, 72].

2.5 RAVEN[®] simulation software

In this section, a brief description of the RAVEN[®] software is given by addressing fundamental aspects and main usages.

The RAVEN[®] simulation software is a software for simulation of composites processing. Using it, it is possible to quickly evaluate temperature and material property evolution of composite laminates on tools. The software comes with a considerable composite material database which makes it suitable for most polymer matrix composites once the fibre and matrix have been combined. It supports both thermoset and thermoplastic matrix materials.

RAVEN[®] can perform simulations in 0D, no spatial dimension, 1D, one spa-

tial dimension, or, 2D, two spatial dimensions. A 0D simulation returns critical material properties as function of time for a prescribed cure cycle at a material point. A 1D simulation allows the evaluation of the effect of tool and part thickness, and heat transfer boundary conditions on the temperature profile and property evolution, through the thickness of a tool-part assembly. A 2D simulation involves all the before mentioned features as well as the possibility of giving shape characteristics to the part.

The software itself is very user friendly. A brief step by step explanation of the 1D analysis is given, as it is the one used for this work:

- The user selects "Thermal profile study" link in the 1D tab in the "Tasks" panel (Figure 2.30);

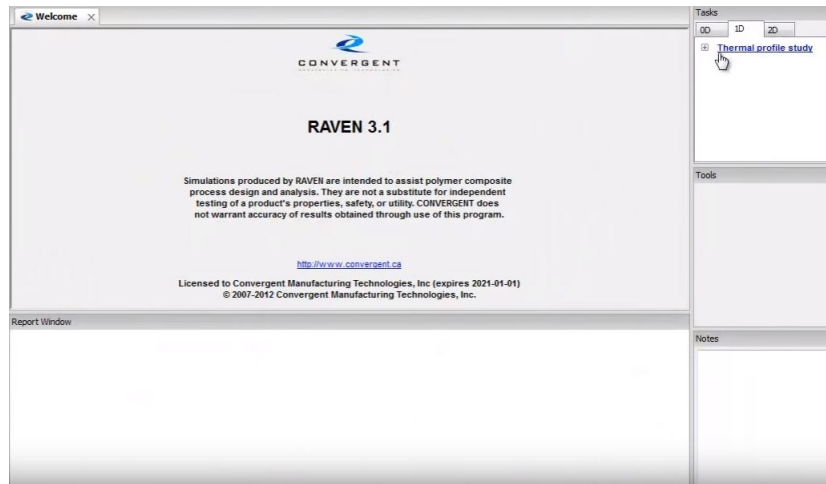


Figure 2.30: 1st explanation figure of the RAVEN[®] software.

- The "create a new thermal profile study" dialogue box appears (Figure 2.31). Here, the user is meant to assign the input conditions, i.e., the desired tool, the different plies of the composite with desired orientations and material type, the type of breather cloth and heat transfer boundary conditions. The thickness of each part is also selected. Figure 2.32 shows a simple stack example.

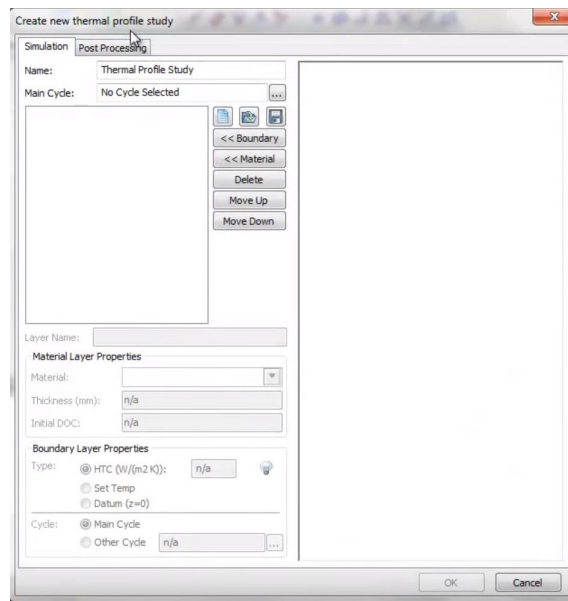


Figure 2.31: 2nd explanation figure of the RAVEN[®] software.

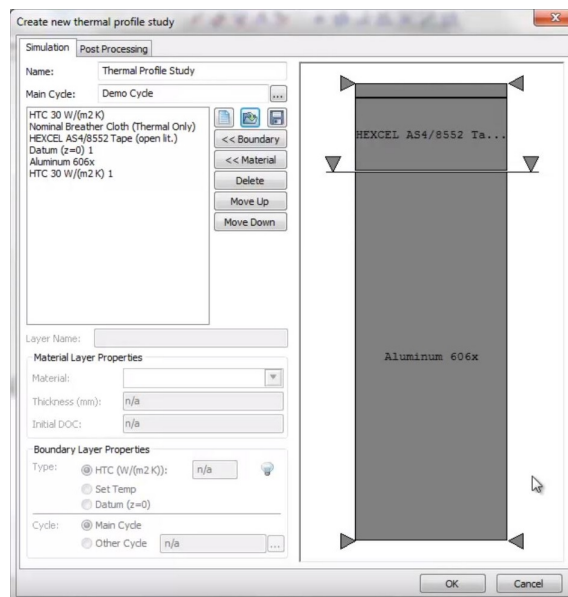


Figure 2.32: 3rd explanation figure of the RAVEN[®] software.

- In the same window, it is mandatory that the user selects or creates a curing cycle. RAVEN[®] has more than one standard cycle for each different material.
- In terms of post processing, the user is able to specify which plots the software will create. It is possible to obtain parameters variation with time our through-thickness of the part (Figure 2.33).

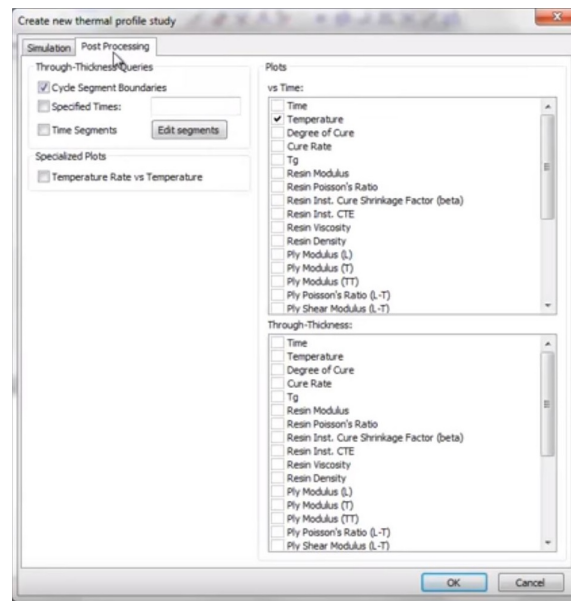


Figure 2.33: 4th explanation figure of the RAVEN[®] software.

- The desired results are shown in a new dialogue box. Figure 2.34 shows the variation of the curing rate and temperature through with time for the composite laminate part.

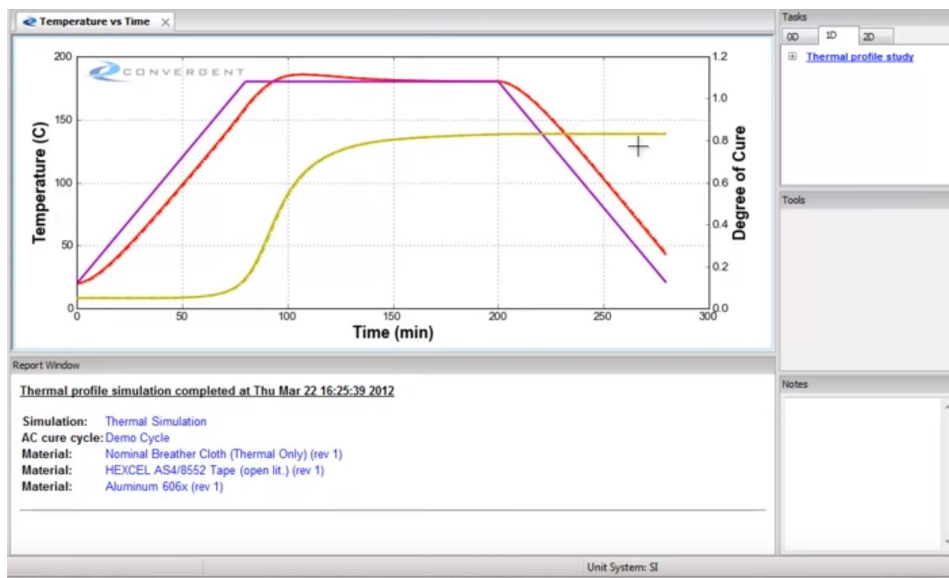


Figure 2.34: 5th explanation figure of the RAVEN[®] software.

Chapter 3

Numerical Simulations

This chapter is dedicated to the numerical simulations of the curing process, of each different manufacturing process, and have the purpose of predicting possible defects on a particular composite laminate part. The simulation will consist in two steps.

The first step consists in the simulation of the curing process in a non FEM environment. The main objective of this step is to numerically obtain the value of the heat transfer coefficient which cures the composite laminate part and generates a laminate and mould temperature distribution that follows the curing temperature one. The software RAVEN[®] is used in this step considering a one-dimensional (1D) analysis, i.e., it is considered that the numerical simulation performed on a through-thickness cross-section of the model is representative of its entire length.

Secondly, knowing the temperature distribution over the surface of the laminate after the curing process, the residual strain due to the pressure and temperature conditions imposed by the process is computed. The purpose of this step is to obtain the strains that are developed during the cure and upon the end of the process, so that the identification of the most crucial areas of their appearance is possible for this particular part. A coupled thermal-displacement simulation is performed in ABAQUS[®].

Finally, with the current state-of-the-art regarding the different manufacturing processes and its most common defects, a qualitative comparison, using two different softwares, is made between Autoclave, RTM and VBO processes in terms of strain concentration tracking and, consequently, possible forming of defects. Figure 3.1 shows a scheme that summarizes mandatory inputs and desirable outputs from both of computational softwares used during this thesis.

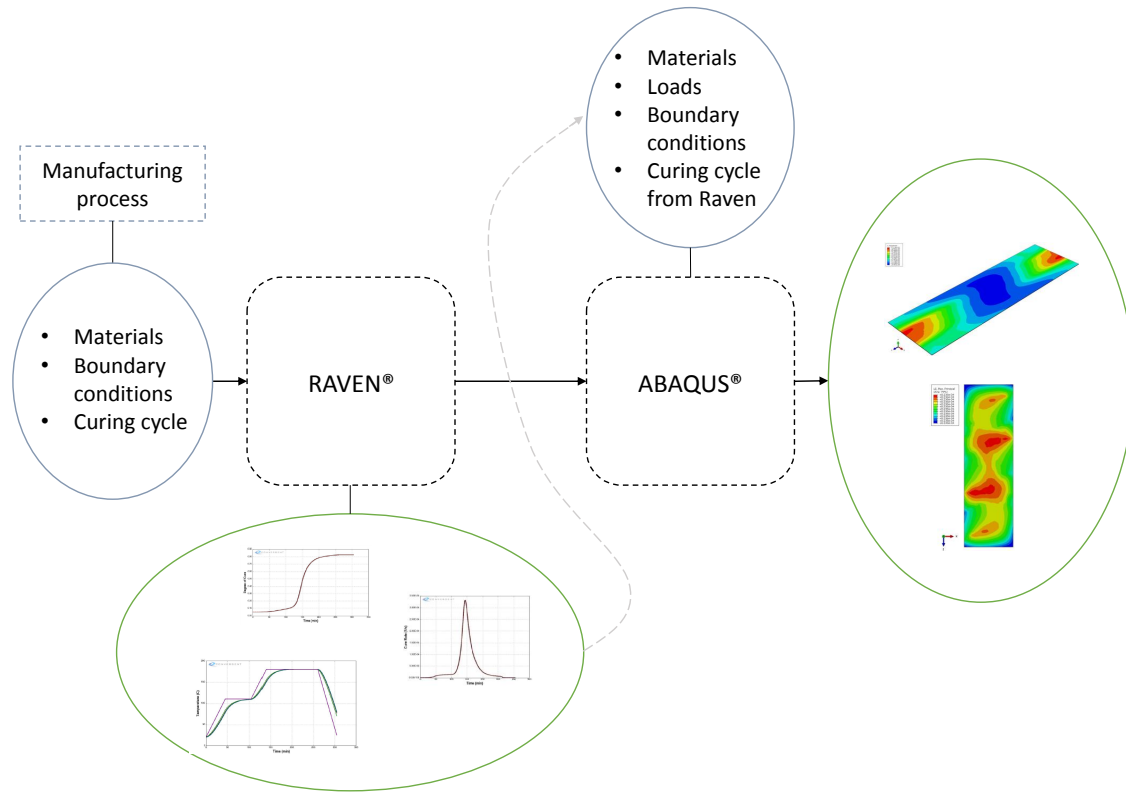


Figure 3.1: Model representation scheme

3.1 Geometry

The model to be analysed is presented in Figure 3.2 and is composed by two parts: i) stringer and ii) skin.

The skin part can be representative of one of a panel of an aircraft and the stringer is the component built in order to avoid incurring large deflection in the skin material. Various shapes and sizes of longitudinal stringers can be used in this design to find which shape of stringer can take more load and resist buckling [73]. For this study, a T type of stringer is used.

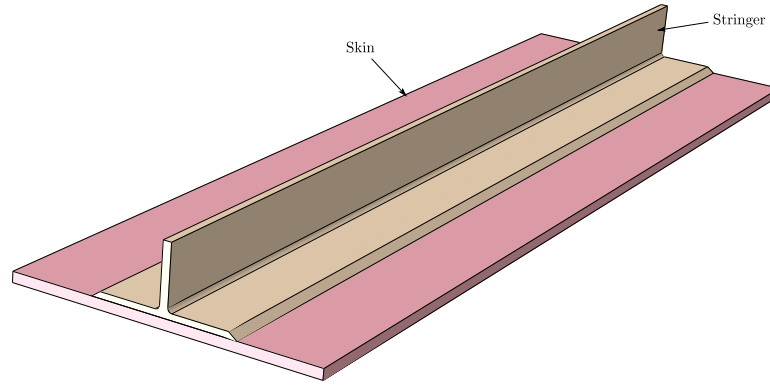


Figure 3.2: Laminate parts

Figure 3.3 shows the in-plane dimensions of the stiffener.

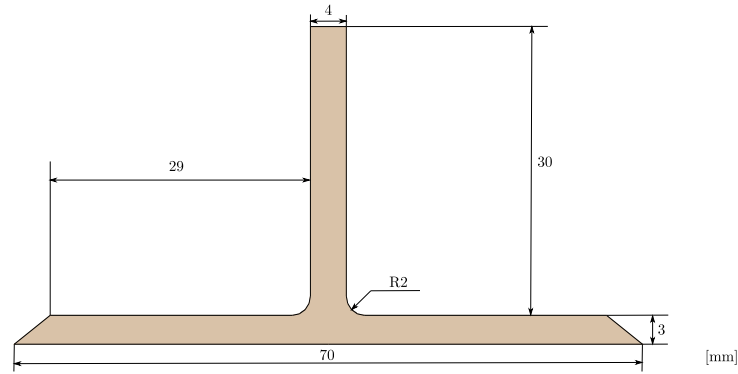


Figure 3.3: Laminate parts

The skin represents a quasi-isotropic $[0^\circ / -45^\circ / 45^\circ / 90^\circ]_s$ eight-ply laminate. Its longitudinal dimension is equal to that of the stiffener and moulds, which is 500 mm. The thickness of each ply is 0.13 mm.

The model is also composed by one mould beneath the part and, for the RTM simulation, a matching mould on top. The lower and upper moulds have a width equal to 520 mm and heights of 1.03 mm and 64.44 mm, respectively. It is assumed that the presence of the stringer does not influence the cure kinetics of the laminate, being a valid assumption simulating the cure process in RAVEN[®] without the stiffener.

3.2 Materials

Three different types of material are used in the numerical simulations. The prepreg AS4/8552 is used for the simulation of the autoclave process. From this material, similar ones were chosen for VBO and RTM. The materials selected were the semipreg IM7/5320-1 (modified resin system created by Cytec to extend out-time and combat associated issues) and a non-crimp fabric (NCF) composite with a HTS

fibre type and a RTM6 epoxy resin, respectively. All three materials chosen have similar fibres and resins, each adequate to the process in use. Both the prepreg and semipreg considered are UD fabrics, which is the reason for the use of the NCF preform.

The necessary material input properties for the finite element analysis of each material of the composite laminate skin are specified in Table 3.1. It is important to note that the material properties used as inputs in the finite element analysis are the ones of an already cured composite.

Table 3.1: Composite laminated skin material properties [23, 24, 25, 26]

Material properties	Autoclave	RTM	VBO
E_{11}^c [MPa]	164000	129550	157133
E_{22}^c [MPa]	12000	7159.3	12060
E_{33}^c [MPa]	12000	7159.3	12060
ν_{12}^c	0.268	0.3125	0.3
ν_{13}^c	0.268	0.3125	0.3
ν_{23}^c	0.44	0.4236	0.45
G_{12}^c [MPa]	5210	1851.7	3590
G_{13}^c [MPa]	5210	1851.7	3590
G_{23}^c [MPa]	3380	1200.1	2410
ρ^c [ton/mm ³]	1.44×10^{-9}	1.555×10^{-9}	2×10^{-9}
c^c [N.mm/(ton.K)]	8.57×10^8	8×10^9	9×10^8
k_{11}^c [W/(mm.K)]	8.41×10^{-4}	4.56×10^{-4}	3.1×10^{-3}
k_{22}^c [W/(mm.K)]	5.4×10^{-5}	4.775×10^{-5}	7×10^{-4}
k_{33}^c [W/(mm.K)]	5.4×10^{-5}	4.775×10^{-5}	7×10^{-4}
α_c^{11} [K ⁻¹]	-1×10^{-7}	2.2×10^{-7}	-5.93×10^{-7}
α_c^{22} [K ⁻¹]	3.1×10^{-7}	-1.8×10^{-7}	5.4×10^{-6}
α_c^{33} [K ⁻¹]	3.1×10^{-7}	-1.8×10^{-7}	5.4×10^{-6}

The ply level properties of the NCF composite, used in the RTM computational model, are obtained through a well known rule of mixtures:

$$E_{11}^c = E_{11}^f \omega_f + E^m (1 - \omega_f) \quad (3.1)$$

$$E_{22}^c = \frac{E_{22}^f E^m}{E_m \omega_f + E_{22}^f (1 - \nu_m^2) (1 - \omega_f)} \quad (3.2)$$

$$\frac{1}{G_{12}^c} = \frac{\omega_f}{G_{12}^f} + \frac{(1 - \omega_f)}{G^m} \quad (3.3)$$

$$\nu_{12}^c = \nu_{12}^f \omega_f + \nu^m (1 - \omega_f) \quad (3.4)$$

$$\rho^c = \omega_f (\rho^f - \rho^m) + \rho^m \quad (3.5)$$

$$k_{11}^c = \omega_f k_{11}^f + (1 - \omega_f) k^m \quad (3.6)$$

$$k_{22}^c = \left(\frac{\omega_f}{k_{22}^f} + \frac{1 - \omega_f}{k_m} \right)^{-1} \quad (3.7)$$

where E_{11}^c , E_{22}^c , G_{12}^c , ν_{12}^c , ρ^c , k_{11}^c and k_{22}^c represent the ply level properties, E_{11}^f , E_{22}^f , G_{12}^f , ρ^f , k_{11}^f and k_{22}^f the fibres properties, E^m , ν^m , G^m , and ρ^m , k^m the matrix properties and ω_f the fibre volume fraction.

According to [74], the coefficients of thermal expansions in the longitudinal direction, α_{11}^c and in the transversal direction, α_{22}^c of the composite laminate can be obtained according to the following expressions:

$$\alpha_{11}^c = \frac{\alpha_{11}^f E_{11}^f \omega_f + \alpha_m E_m (1 - \omega_f)}{\omega_f E_{11}^f + E_m (1 - \omega_f)} \quad (3.8)$$

$$\alpha_{22}^c = (1 + \nu_m) \alpha_m (1 - \omega_f) \alpha_{22}^f \omega_f + \alpha_{11}^f \nu_{12}^f \omega_f - \alpha_{11}^c (\nu_{12}^f \omega_f + \nu_m (1 - \omega_f)) \quad (3.9)$$

where α_m is the CTE of the matrix and α_{11}^f and α_{22}^f are the fibres longitudinal and transversal CTEs, respectively.

Figure 3.4 represents the former equations, where the properties of the constituents are reported in [20, 18].

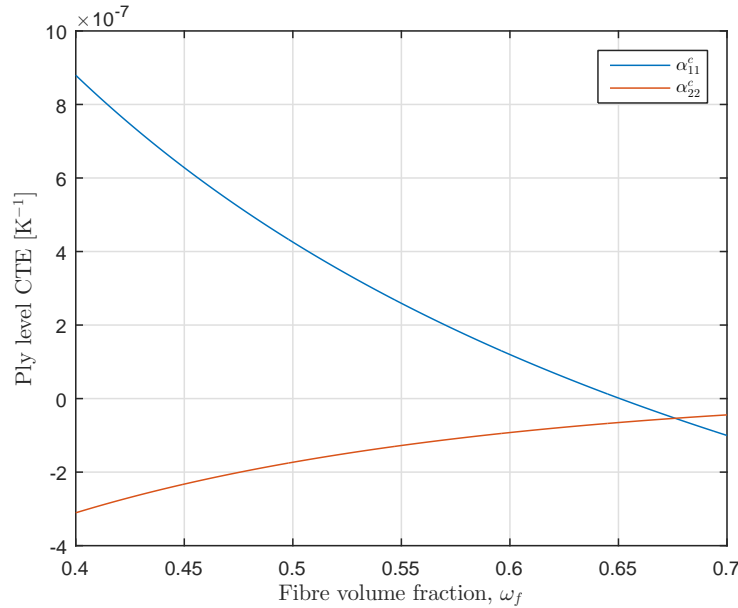


Figure 3.4: Variation of the CTE with fibre volume fraction for the reported constituents [18, 19, 20, 21].

The reported material properties that are meant to be used in the autoclave and VBO simulations were reported for a ω_f of approximately 0.55, so, according to Figure 3.4, the CTE in the longitudinal and transversal directions of the material used for the VBO process are $2.2 \times 10^{-7} \text{ K}^{-1}$ and $-1.8 \times 10^{-7} \text{ K}^{-1}$, respectively.

The type of moulds used throughout the analyses are Invar 36, a 36% nickel-iron alloy possessing a rate of thermal expansion approximately one-tenth that of carbon steel. This material has already been used in former works [75, 76, 77]. The material properties of the mould are specified in Table 3.2.

Table 3.2: Invar 36 material properties [27]

Material properties	Value
E_I [MPa]	140000
ν_I	0.3
ρ_I [ton/mm ³]	2.768×10^{-8}
c_I [N.mm/(ton.K)]	5.1×10^8
k_I [W/(mm.K)]	1.05×10^{-2}
α_I [K ⁻¹]	6×10^{-7}

For simplicity, the stringer is assumed to be made of steel. Its material properties are specified in Table 3.3.

Table 3.3: Stiffener material properties

Material properties	Value
E_s [MPa]	210000
ν_s	0.33
ρ_s [ton/mm ³]	8.05×10^{-9}
c_s [N.mm/(ton.K)]	4.90×10^8
k_s [W/(mm.K)]	5.02×10^{-2}
α_s [K ⁻¹]	1.08×10^{-5}

3.3 Step I - RAVEN[®]

In this section, simulations using RAVEN[®] software are performed. With the the adequate boundary conditions and material properties, a deep analysis is made for the autoclave and VBO manufacturing processes. Since the material properties of the NCF composite are obtained based on its constituents, it is impossible to perform a simulation using a software which only has a material database of ply level material properties, so the RTM curing process is not simulated.

3.3.1 Autoclave

Figure 3.5 shows the layup stacking sequence, the mould and the applied boundary conditions for the autoclave process in the RAVEN[®] environment.

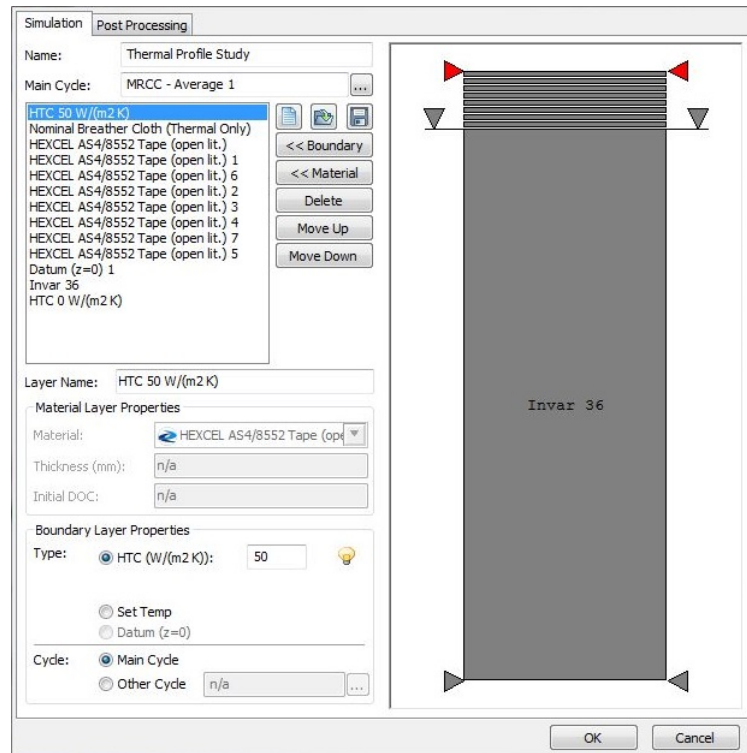


Figure 3.5: Autoclave model setup in Raven®.

The temperature distribution used for the curing process is a two hold cycle and is represented in Figure 3.6.

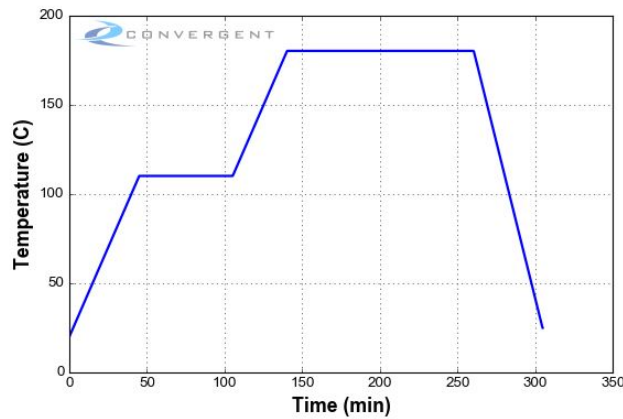


Figure 3.6: Curing temperature distribution of the autoclave model.

First, the influence of the heat transfer coefficient is analysed. Three different admissible values were used: 20 W/m²K, 40 W/m²K and 80 W/m²K [78, 79]. Figures 3.7 represent the variation of the temperature throughout the curing cycle of the mould and the laminate.

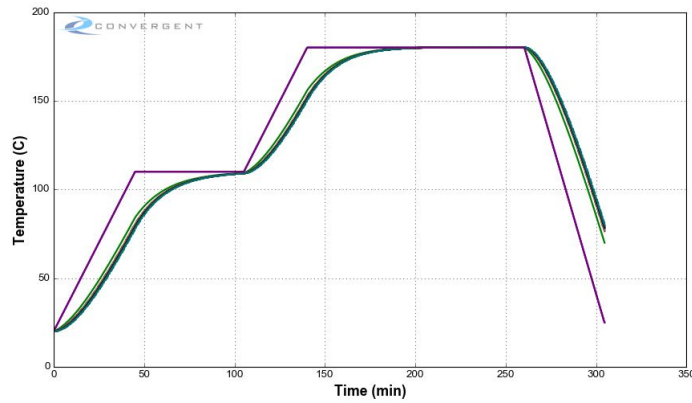
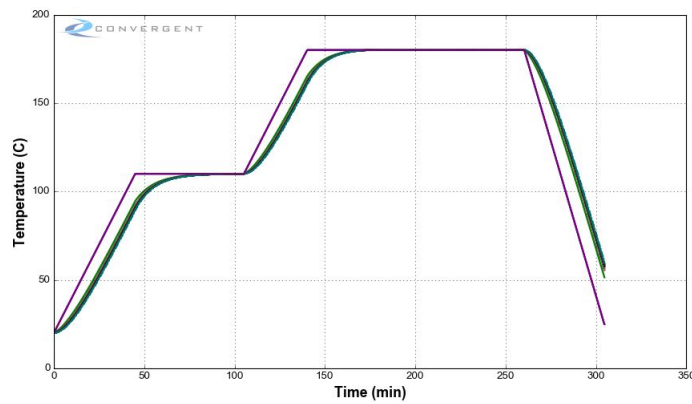
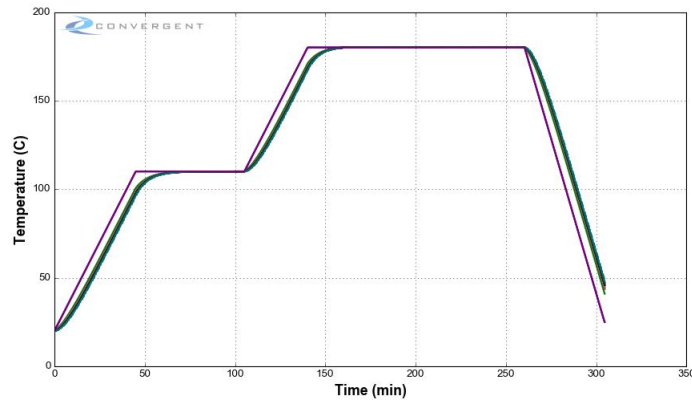
(a) $h = 20 \text{ W/m}^2\text{K}$ (b) $h = 40 \text{ W/m}^2\text{K}$ (c) $h = 80 \text{ W/m}^2\text{K}$

Figure 3.7: Mould and laminate temperature vs curing temperature distribution for the autoclave process for different values of h .

With the results obtained, it is concluded that, for a heat coefficient of $80 \text{ W/m}^2\text{K}$ the temperature of the composite laminate part follows the temperature distribution of the curing cycle best. Hence, in the finite element simulations, the temperature is applied in an equally distributed manner throughout the model.

Figures 3.8-3.9 represent the degree of cure and the cure rate of the skin during the curing cycle.

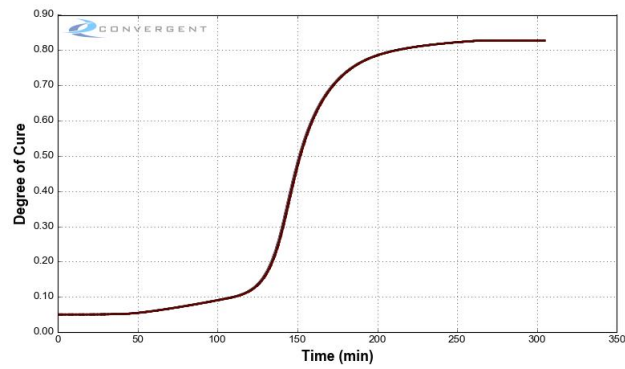


Figure 3.8: Degree of cure of AS4/8552 during curing cycle for $h = 80 \text{ W/m}^2 \text{ K}$.

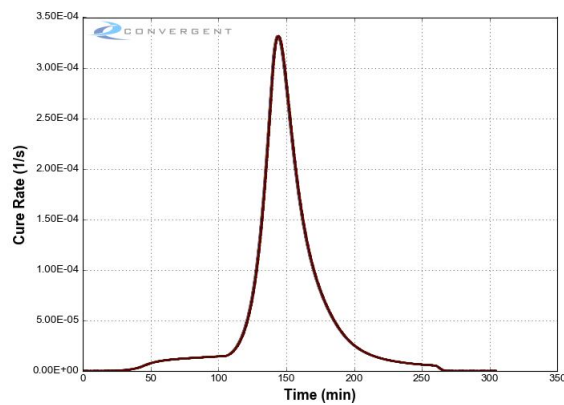


Figure 3.9: Cure rate of AS4/8552 during curing cycle, for $h = 80 \text{ W/m}^2 \text{ K}$.

3.3.2 VBO

Figure 3.10 shows the layup stacking sequence, the mould and the applied boundary conditions for the autoclave process in the RAVEN® environment.

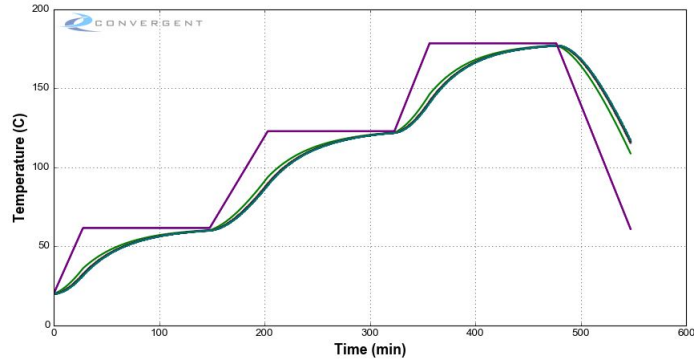
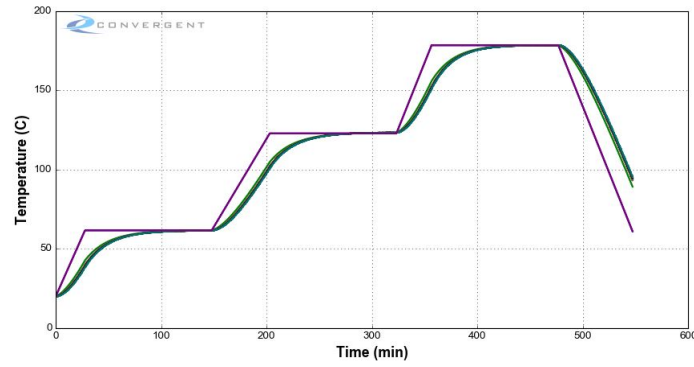
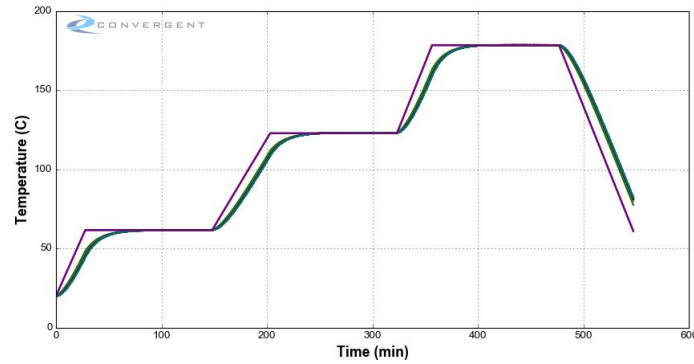
(a) $h = 20 \text{ W/m}^2\text{K}$ (b) $h = 30 \text{ W/m}^2\text{K}$ (c) $h = 50 \text{ W/m}^2\text{K}$

Figure 3.12: Mould and laminate temperature vs curing temperature distribution for the VBO process for different values of h .

Comparing the distributions, it is clear that, for a value of $50 \text{ W/m}^2\text{K}$, the temperatures of each ply and mould follow the temperature distributions of the curing cycle temperature.

Figures 3.13-3.14 represent the degree of cure and the cure rate of the skin during the curing cycle.

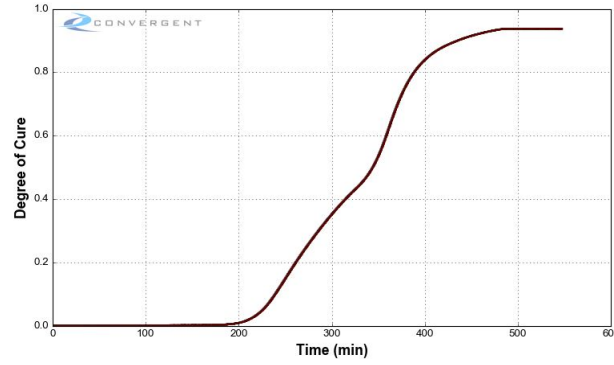


Figure 3.13: Degree of cure of IM7/5320-1 during curing cycle for $h = 50 \text{ W/m}^2\text{K}$.

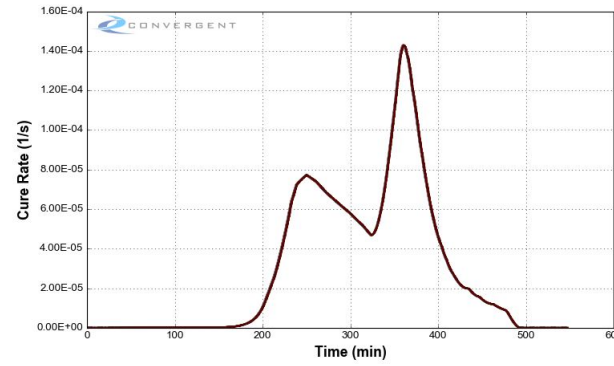


Figure 3.14: Cure rate of IM7/5320-1 during curing cycle for $h = 50 \text{ W/m}^2\text{K}$.

3.3.3 Results and discussion

This step was fundamental in order to obtain a valid value for the heat transfer coefficient to be used in the finite element simulations. RAVEN[®] software showed to be a powerful tool to obtain the optimum values for the heat coefficient, those being $80 \text{ W/m}^2\text{K}$ and $50 \text{ W/m}^2\text{K}$ for the autoclave and VBO processes, respectively.

With the aforementioned values for the heat transfer coefficients, according to both Figure 3.7 and 3.12, both materials showed a fully cured behaviour at the end of the curing process. However, the distributions of the curing rate are slightly different from one another. This is due to the difference in the temperature distribution of the curing cycle. AS4/8552, which was submitted to a two hold temperature curing cycle, reached a maximum in its cure rate as soon as the curing cycle temperature reached its maximum magnitude. Then, it rapidly decreased due to the holding branch of the temperature distribution. AS4/5250-1, presented two relative maximums in the cure rate distributions, since the temperature of the curing cycle represents a three hold cycle, generating a slightly different distribution of the degree of cure throughout time.

3.4 Step II - Finite element modelling

In this section, a coupled temperature displacement simulation is performed using ABAQUS® software, in order to evaluate the location of strain gradients in the composite laminate and, consequently, the possible appearances of defects.

The autoclave, VBO and RTM finite element models are outlined in Figures 3.15 and 3.16. The main difference between the model of the autoclave and the one of the VBO is in the pressure applied to the laminate, since, in the autoclave, pressure is applied out of the part/mould assembly.

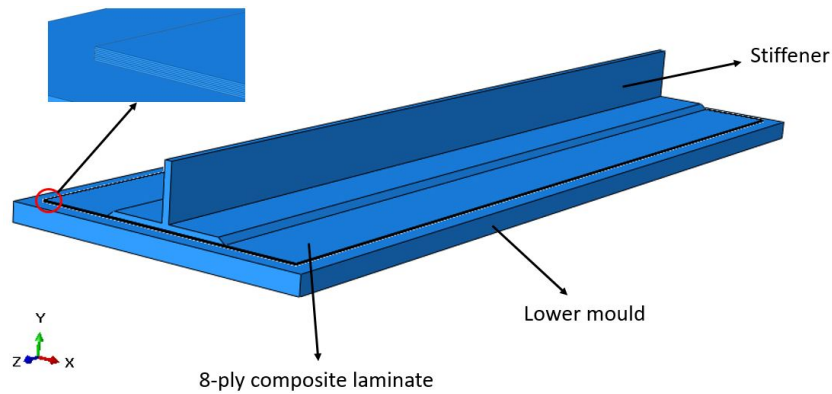


Figure 3.15: Autoclave and VBO computational models and evidence of the eight plies.

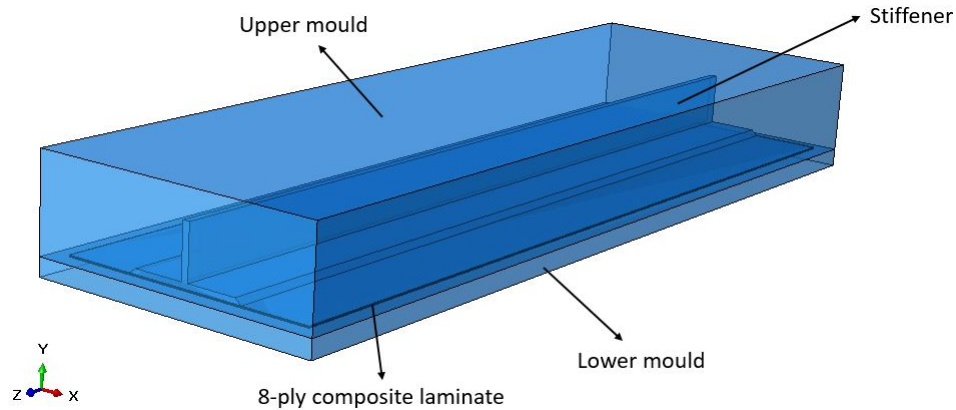


Figure 3.16: RTM computational model.

The composite laminate, the lower mould and the stringer are modelled by means of a C3D20RT, A 20-node thermally coupled brick, triquadratic displacement, trilinear temperature with reduced integration. However, since the upper mould in the RTM model represents a complex geometrical part, it is modelled by means of a C3D10MT, a 10-node modified thermally coupled second-order tetrahedron with hourglass control. All elements have an average size of 3 mm, having the autoclave and VBO models a total of 102562 elements and the RTM model 241095 elements.

The interactions between parts are modelled using a surface-to-surface contact interaction with a penalty friction formulation with a coefficient of 0.2, 0.6 and 0.65 in-between plies, between the laminate and the stiffener and between the lower and upper mould, respectively. A normal behaviour is imposed with a "Hard" Contact in Pressure-Overclosure and default relationships are used in the "Heat generation" options: i) the fraction of dissipated energy caused by friction or electric currents that is converted to heat is 1 and ii) the fraction of converted heat distributed to slave surface is equal to 0.5.

Since the RTM manufacturing process implies a resin impregnation phase, which a structural model cannot simulate, a computational fluid dynamics environment would be recommended. The present simulation exclusively involves the cure process step, i.e., the phase where both moulds and the part to be processed are submitted to the cure temperature distribution recommended in the resin manufacturer datasheet.

3.4.1 Autoclave

In this subsection, the boundary conditions and the numerical results regarding the autoclave computational model are outlined.

In the present simulation, the pressure and temperature distributions are applied in the same step. The temperature follows the distribution represented in Figure 3.6 and the pressure distribution is the one presented in Figure 3.17.

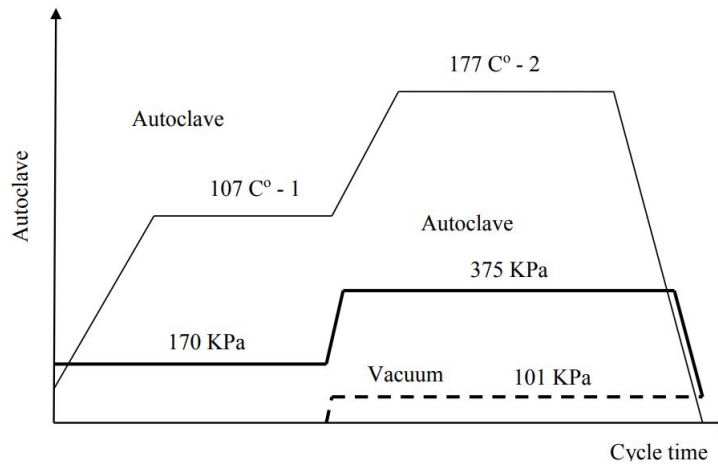


Figure 3.17: Pressure load distribution applied during curing process in the autoclave model.

The loads and boundary conditions applied to the model are represented in Figure 3.18.

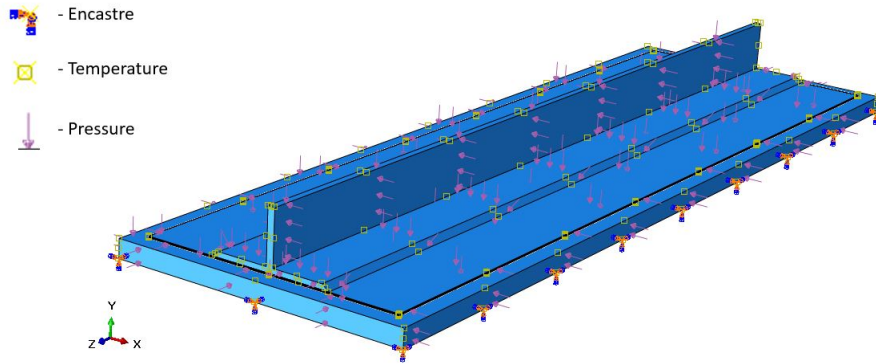


Figure 3.18: Loads and BC applied to the autoclave computational model.

As Figure 3.18 depicts, the lower surface of the mould is completely fixed, i.e., all degrees of freedom are restrained ($u_x = u_y = u_z = \theta_x = \theta_y = \theta_z = 0$), pressure is applied in the upper part of the model and temperature BC is applied to all the surfaces of the model.

Figures 3.19-3.34 show the strain and stress (MPa) distribution in the different plies of the composite laminate after the autoclave curing process.

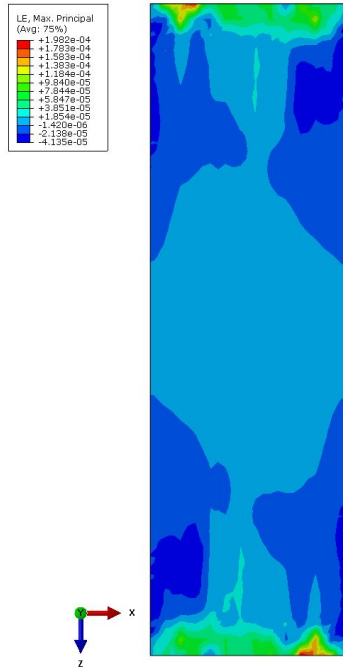


Figure 3.19: Strain distribution in the first ply after the curing process.

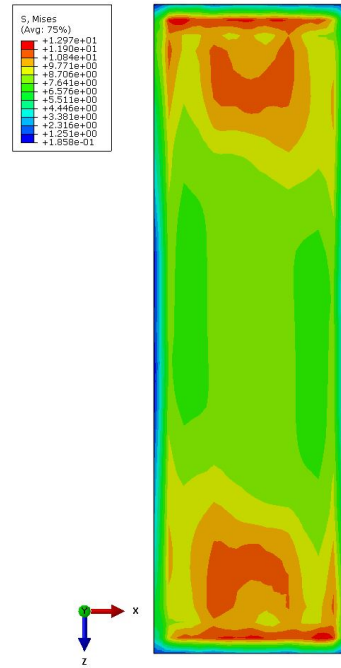


Figure 3.20: Stress distribution in the first ply after the curing process.

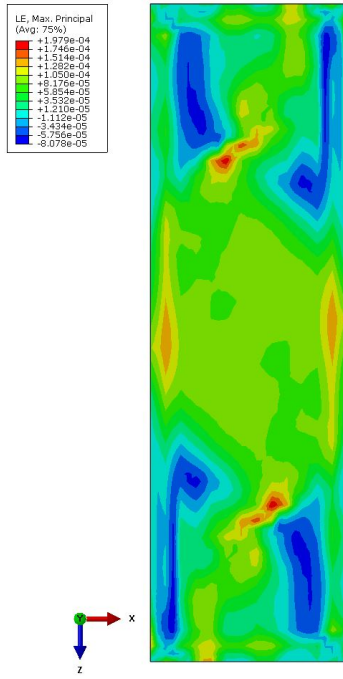


Figure 3.21: Strain distribution in the second ply after the curing process.

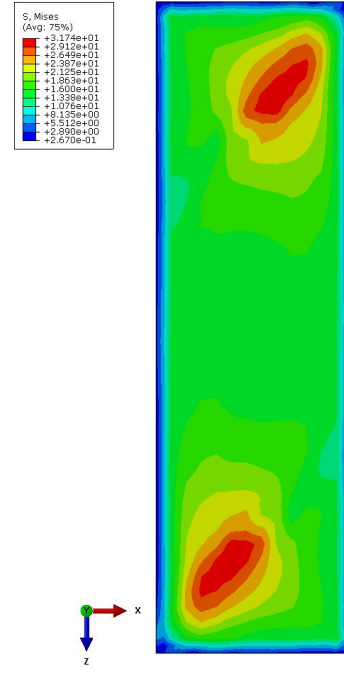


Figure 3.22: Stress distribution in the second ply after the curing process.

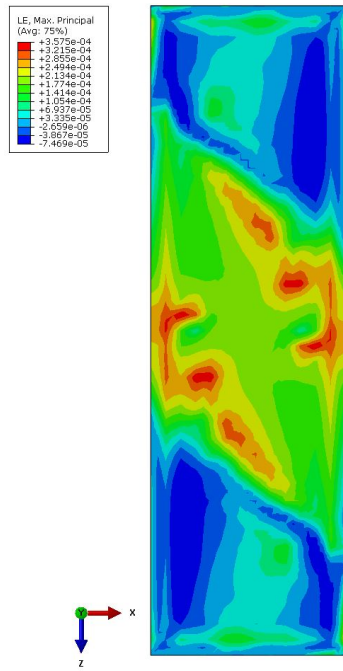


Figure 3.23: Strain distribution in the third ply after the curing process.

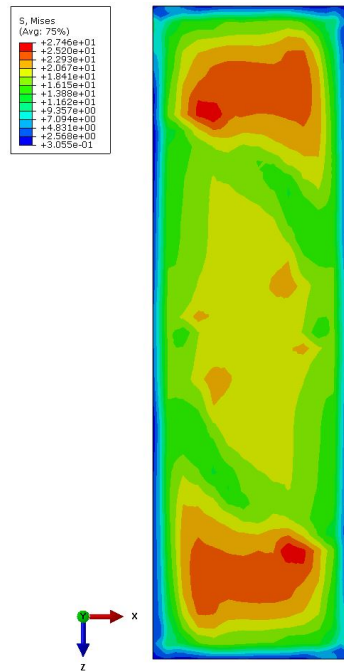


Figure 3.24: Stress distribution in the third ply after the curing process.

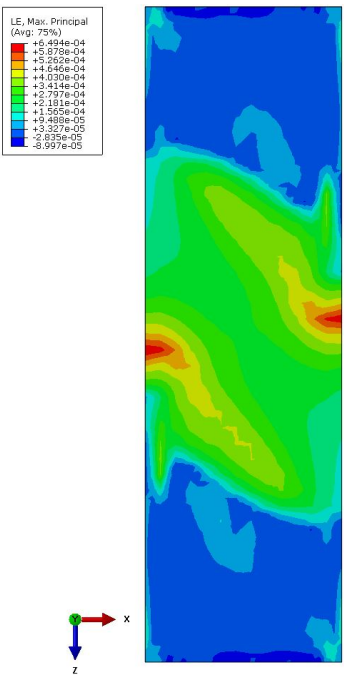


Figure 3.25: Strain distribution in the fourth ply after the curing process.

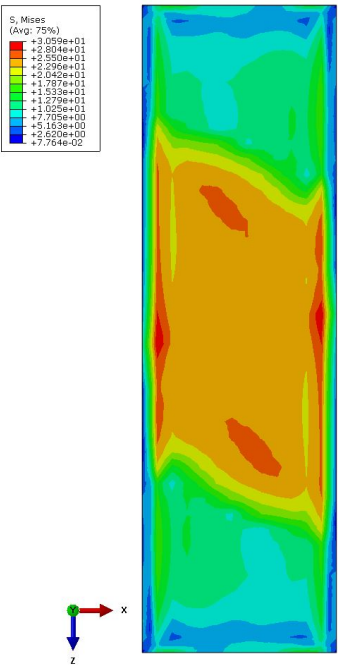


Figure 3.26: Stress distribution in the fourth ply after the curing process.

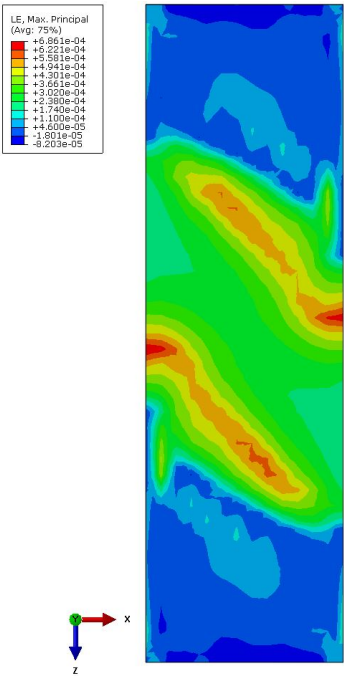


Figure 3.27: Strain distribution in the fifth ply after the curing process.

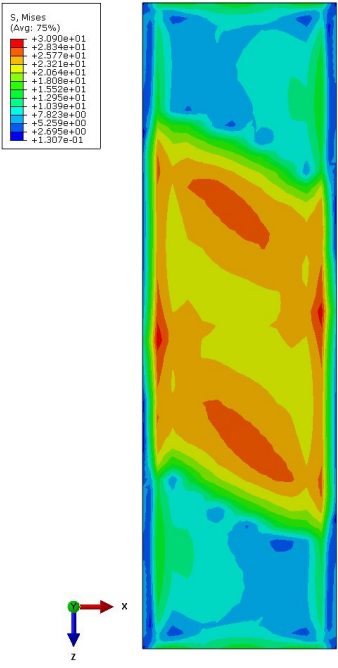


Figure 3.28: Stress distribution in the fifth ply after the curing process.

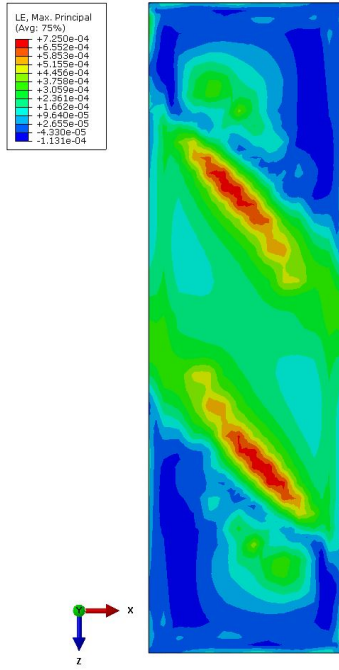


Figure 3.29: Strain distribution in the sixth ply after the curing process.

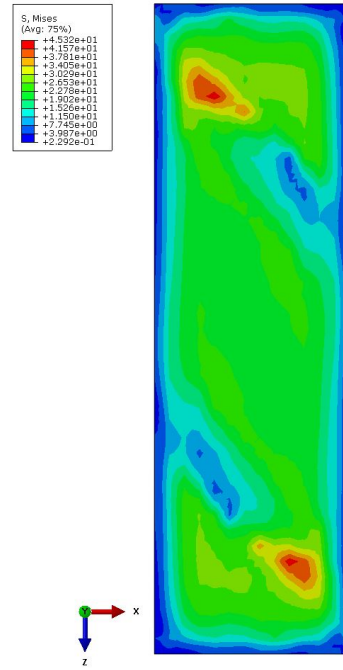


Figure 3.30: Stress distribution in the sixth ply after the curing process.

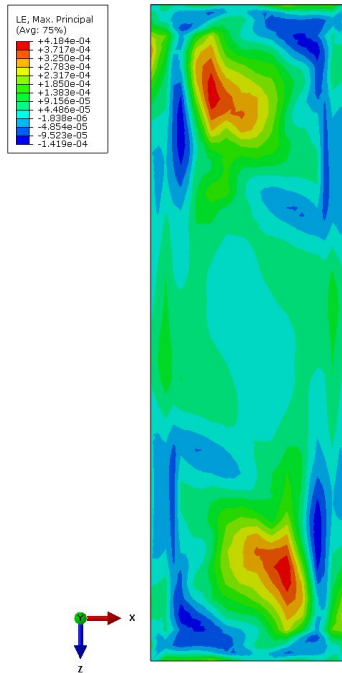


Figure 3.31: Strain distribution in the seventh ply after the curing process.

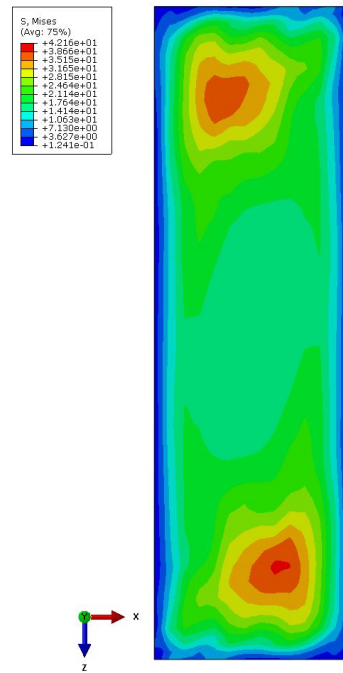


Figure 3.32: Stress distribution in the seventh ply after the curing process.

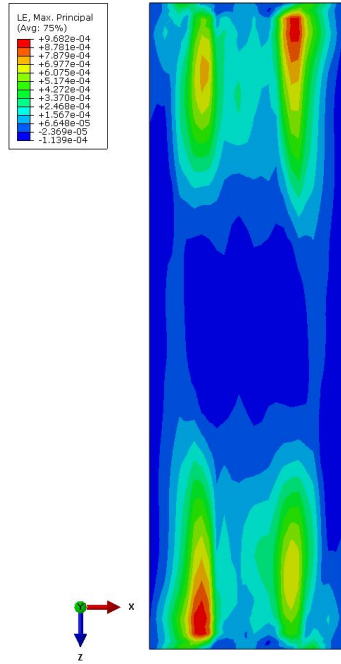


Figure 3.33: Strain distribution in the eighth ply after the curing process.

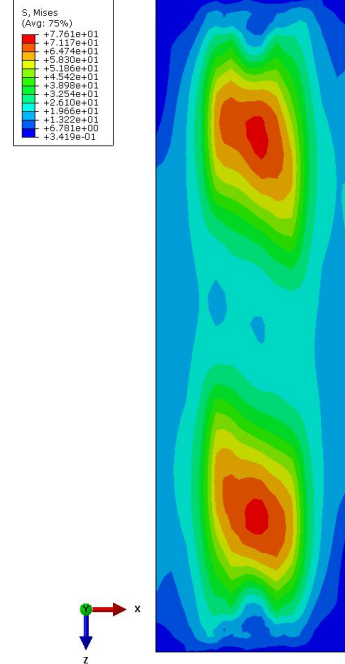


Figure 3.34: Stress distribution in the eighth ply after the curing process.

3.4.2 RTM

In this subsection, the boundary conditions and the numerical results regarding the RTM computational model are outlined.

This computational model is only submitted to the temperature profile after the impregnation phase. The cure cycle, according to McIlhagger et al. [22] is detailed in Figure 3.35.

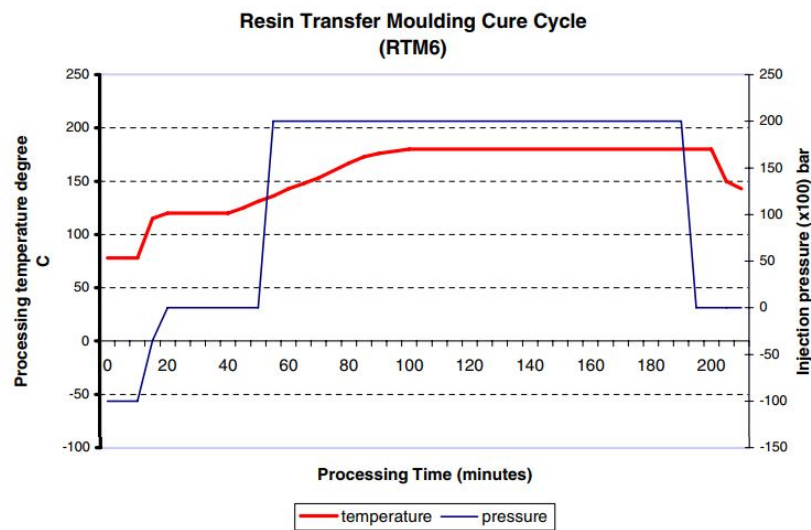


Figure 3.35: RTM 6 cure cycle for composite manufacture [22].

As it has been stated, the values meant to be used for the heat transfer coefficient in this computational model are impossible to obtain using the aforementioned software. As a result, similar values to those of the other processes analysed are used for the exterior of the mould and for the in between of the mould and the skin and stiffener. 30 W/m^2 is used for in between plies and 80 W/m^2 for the outside of the mould.

The loads and boundary conditions applied to the model are represented in Figure 3.36.

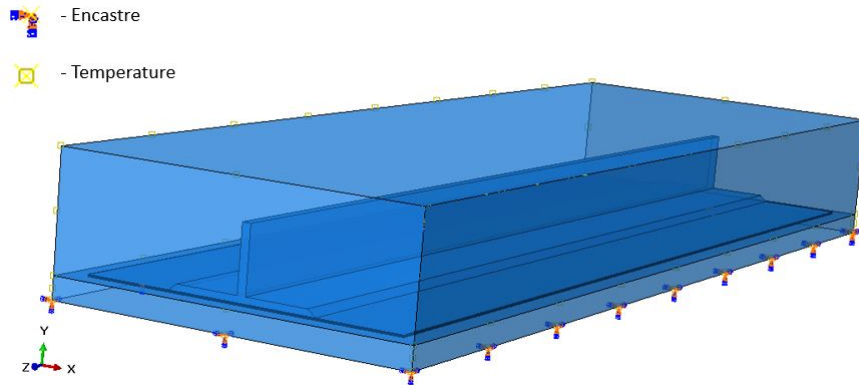


Figure 3.36: Loads and BC applied to the RTM computational model.

The same "encastre" BC is applied to prevent the model's movement, and a uniform temperature BC is applied to all of the exterior surfaces of the moulds.

Figures 3.37-3.52 show the strain and stress (MPa) distribution in the various plies of the composite laminate after the RTM curing process.

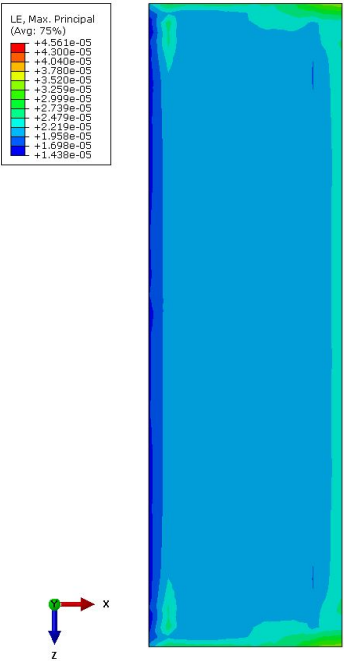


Figure 3.37: Strain distribution in the first ply after the curing process.

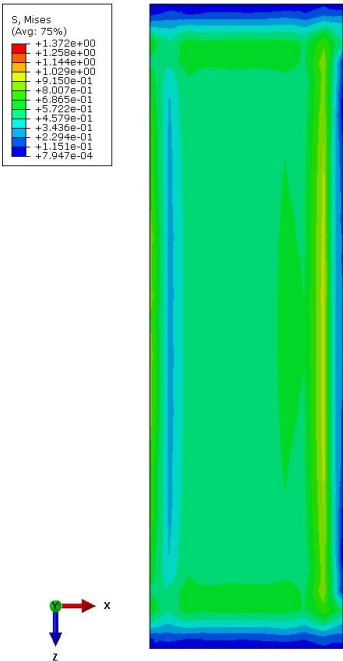


Figure 3.38: Stress distribution in the first ply after the curing process.

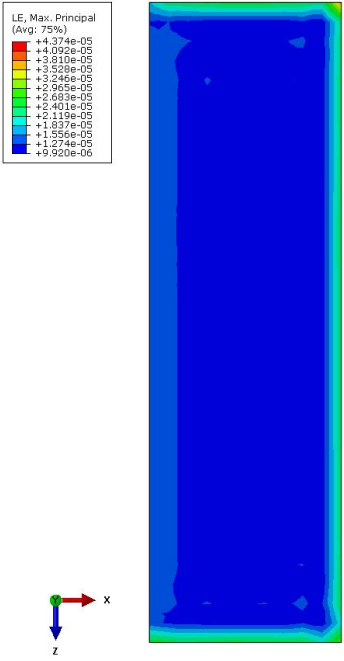


Figure 3.39: Strain distribution in the second ply after the curing process.

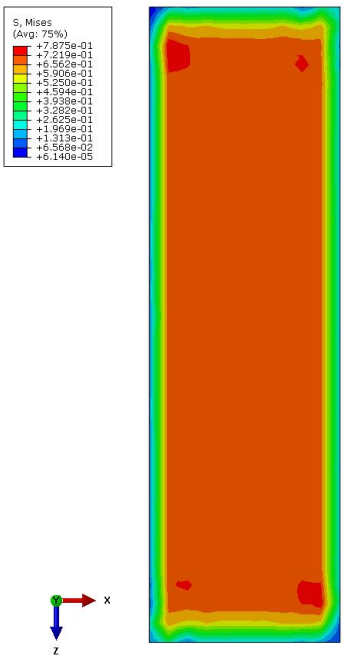


Figure 3.40: Stress distribution in the second ply after the curing process.

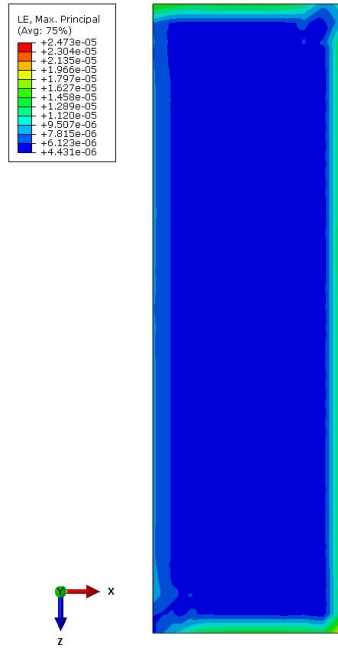


Figure 3.41: Strain distribution in the third ply after the curing process.

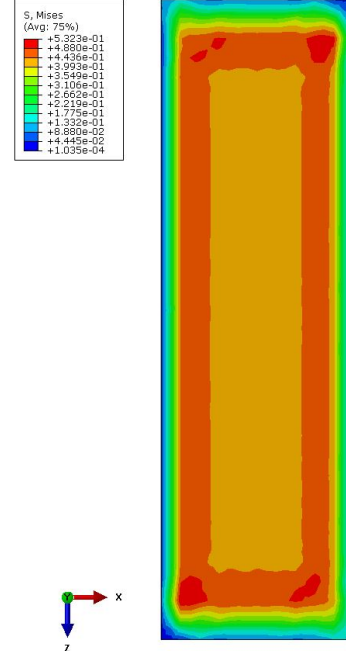


Figure 3.42: Stress distribution in the third ply after the curing process.

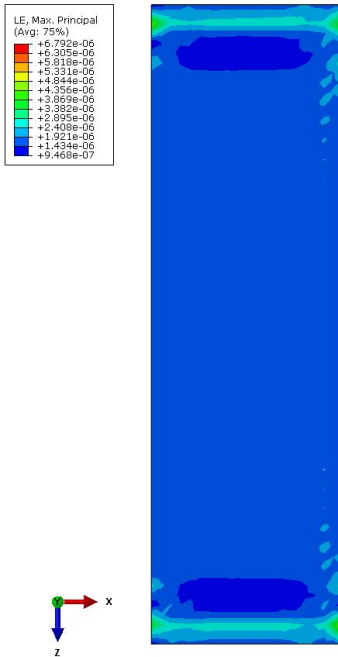


Figure 3.43: Strain distribution in the fourth ply after the curing process.

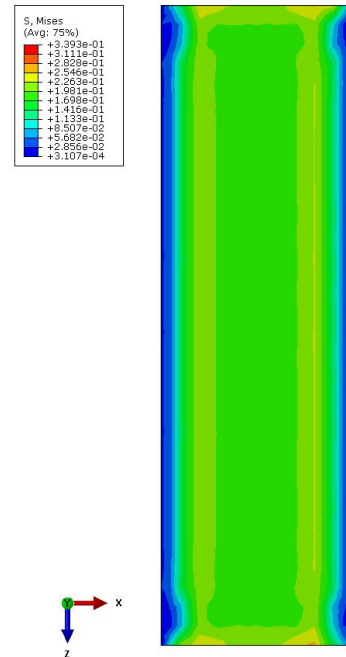


Figure 3.44: Stress distribution in the fourth ply after the curing process.

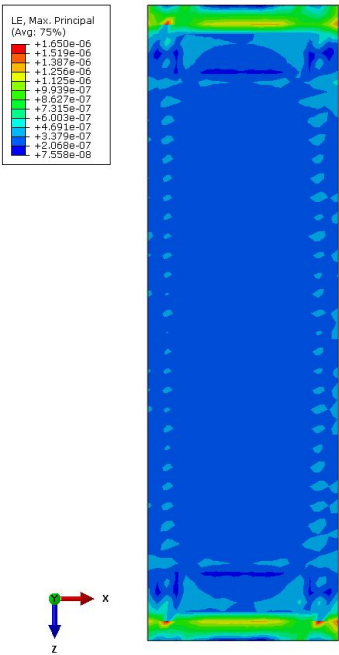


Figure 3.45: Strain distribution in the fifth ply after the curing process.

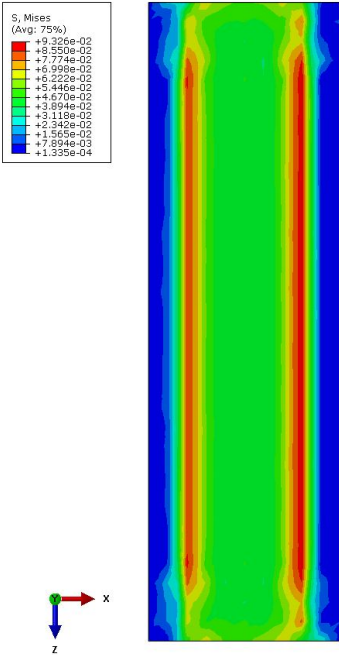


Figure 3.46: Stress distribution in the fifth ply after the curing process.

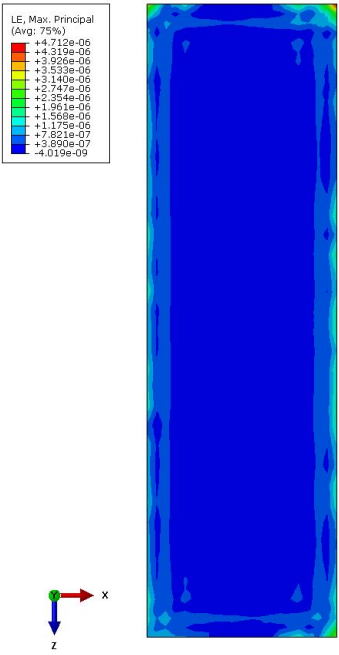


Figure 3.47: Strain distribution in the sixth ply after the curing process.

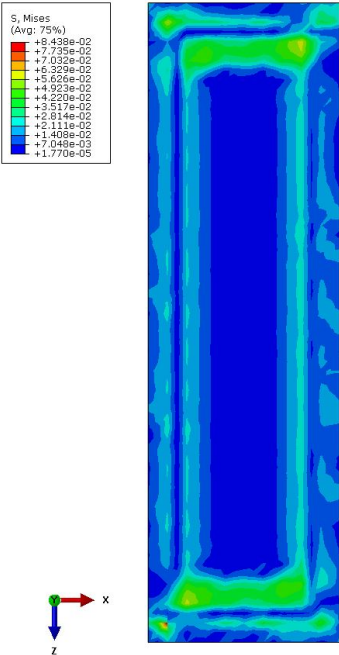


Figure 3.48: Stress distribution in the sixth ply after the curing process.

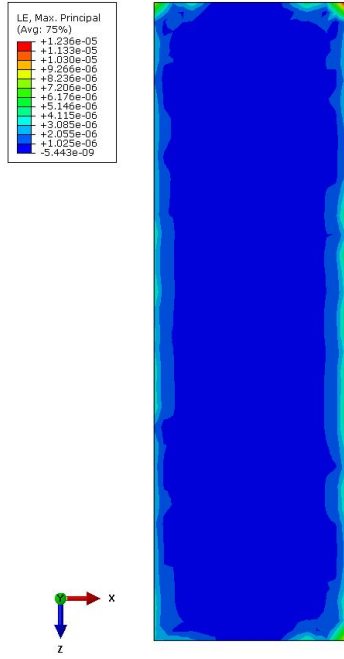


Figure 3.49: Strain distribution in the seventh ply after the curing process.

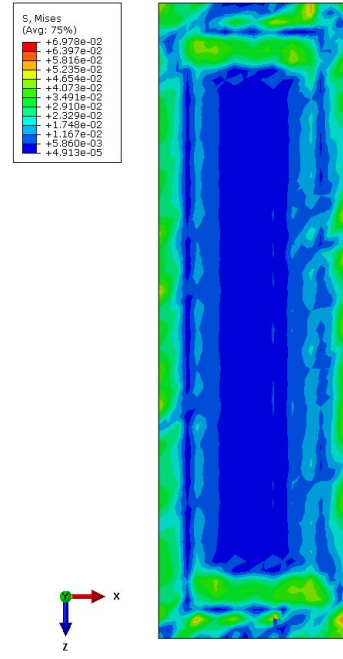


Figure 3.50: Stress distribution in the seventh ply after the curing process.

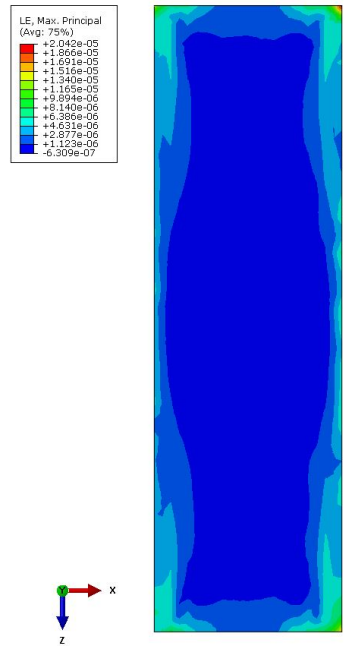


Figure 3.51: Strain distribution in the eighth ply after the curing process.

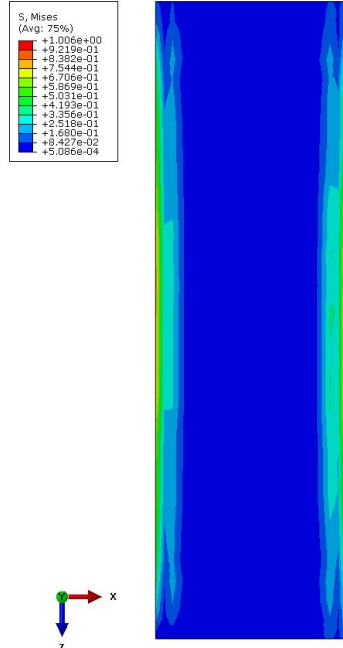


Figure 3.52: Stress distribution in the eighth ply after the curing process.

3.4.3 VBO

In this subsection, the boundary conditions and the numerical results regarding the VBO computational model are outlined.

In the VBO simulation only a temperature distribution is applied. The temperature has the same distribution as the one represented in Figure 3.11.

The loads and boundary conditions applied to the model are represented in Figure 3.53.

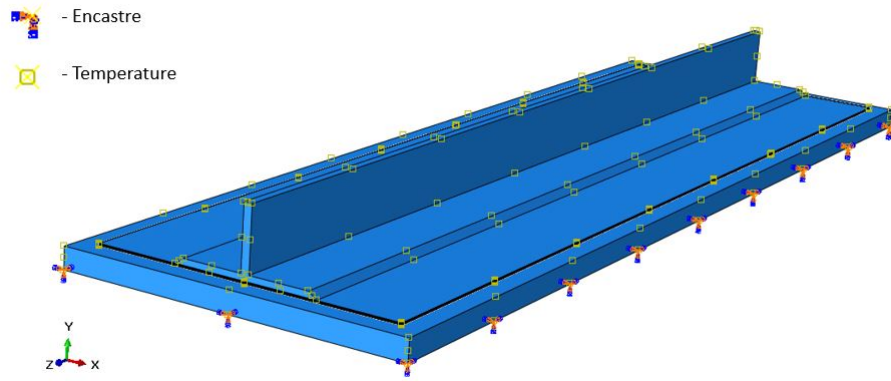


Figure 3.53: Loads and BC applied to the VBO computational model.

The same "encastre" BC is applied to prevent the mould movement and a uniform temperature BC is applied to all of the surfaces of the model.

Figures 3.54-3.69 show the strain and stress (MPa) distribution in the various plies of the composite laminate after the VBO curing process.

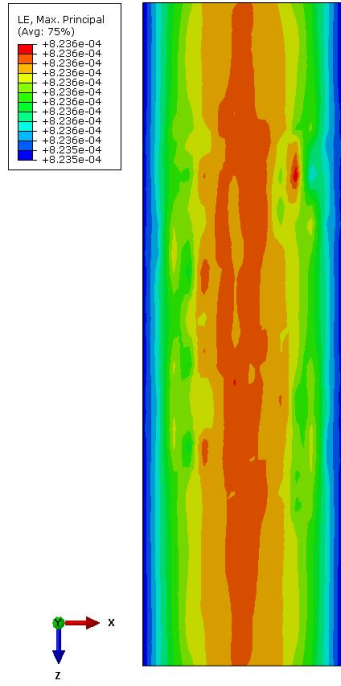


Figure 3.54: Strain distribution in the first ply after the curing process.

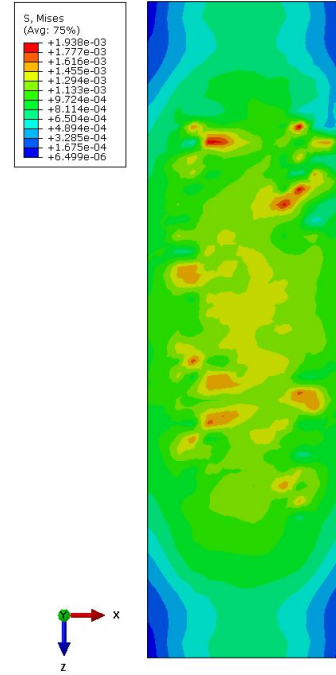


Figure 3.55: Stress distribution in the first ply after the curing process.

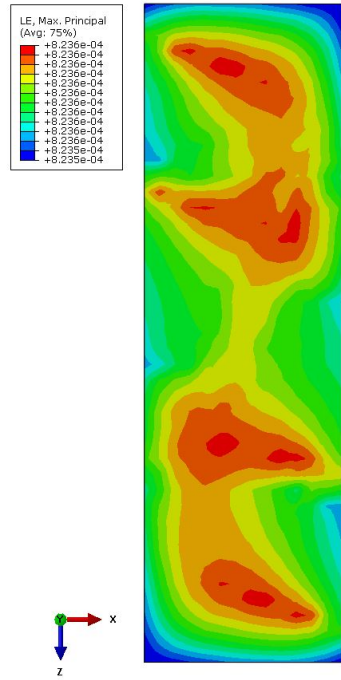


Figure 3.56: Strain distribution in the second ply after the curing process.

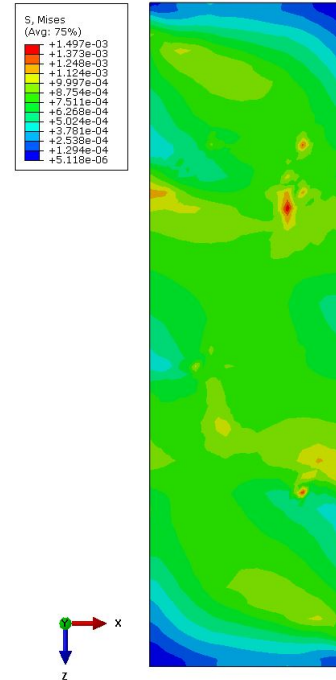


Figure 3.57: Stress distribution in the second ply after the curing process.

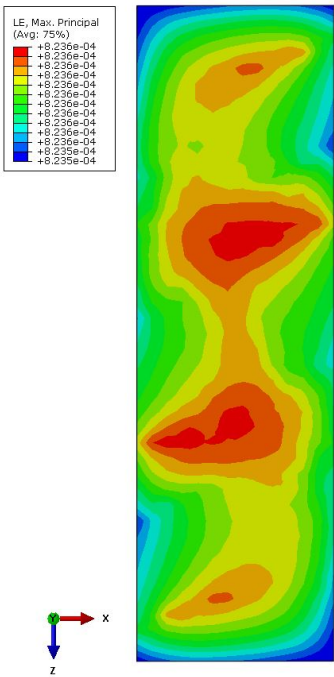


Figure 3.58: Strain distribution in the third ply after the curing process.

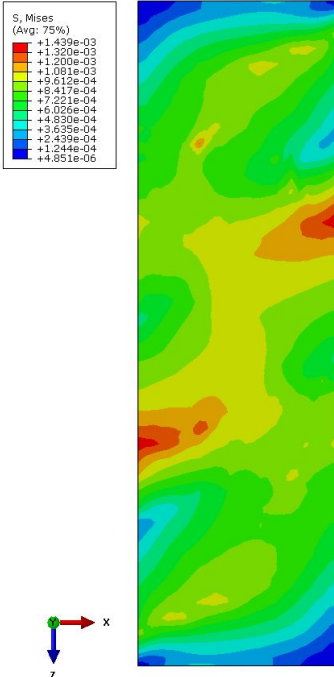


Figure 3.59: Stress distribution in the third ply after the curing process.

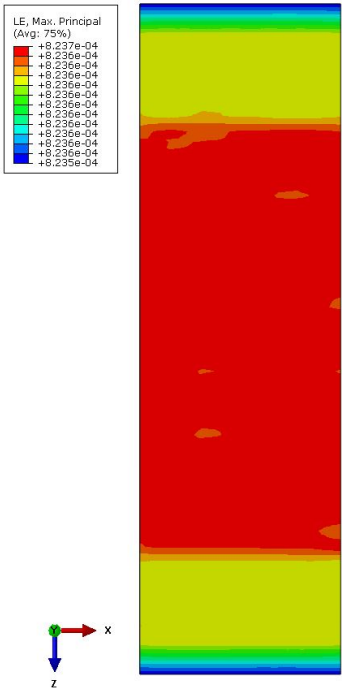


Figure 3.60: Strain distribution in the fourth ply after the curing process.

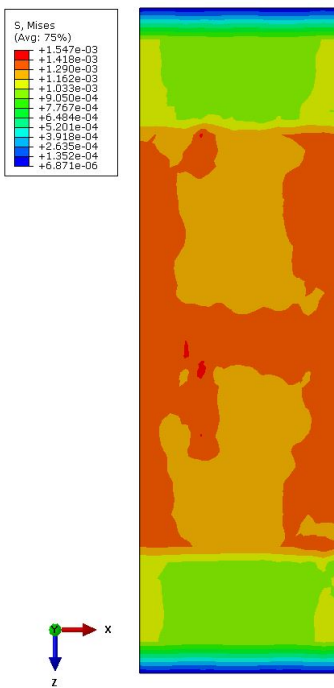


Figure 3.61: Stress distribution in the fourth ply after the curing process.

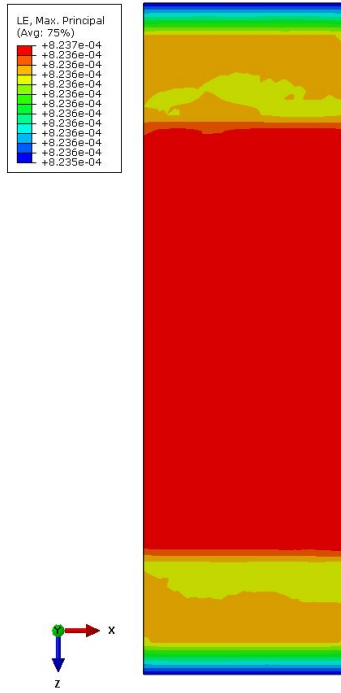


Figure 3.62: Strain distribution in the fifth ply after the curing process.

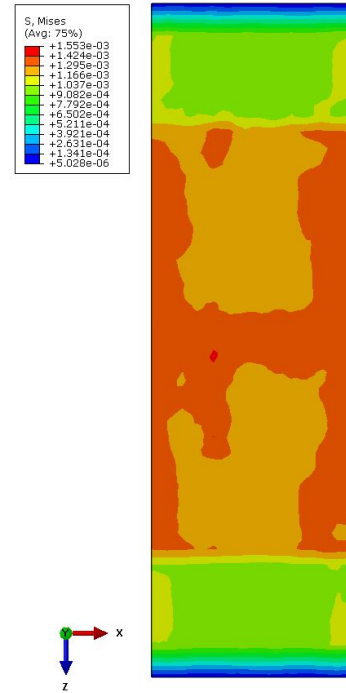


Figure 3.63: Stress distribution in the fifth ply after the curing process.

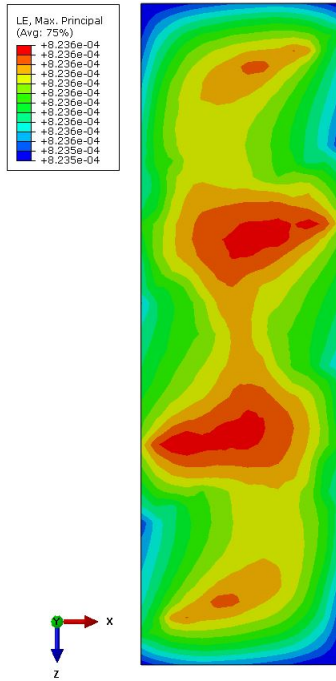


Figure 3.64: Strain distribution in the sixth ply after the curing process.

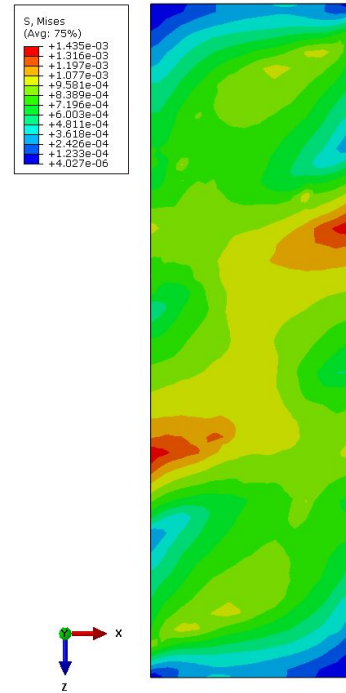


Figure 3.65: Stress distribution in the sixth ply after the curing process.

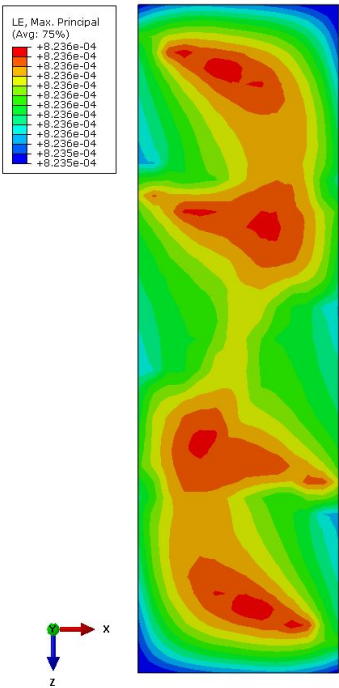


Figure 3.66: Strain distribution in the seventh ply after the curing process.

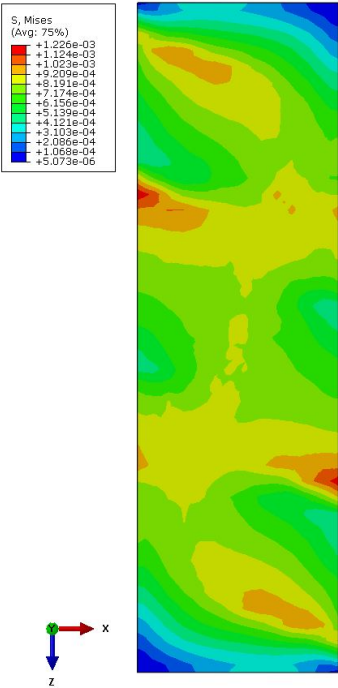


Figure 3.67: Stress distribution in the seventh ply after the curing process.

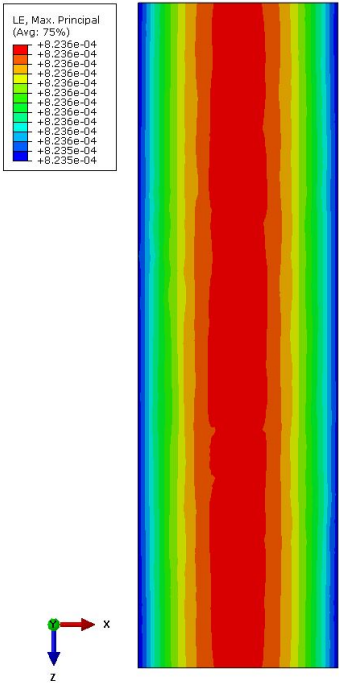


Figure 3.68: Strain distribution in the eighth ply after the curing process.

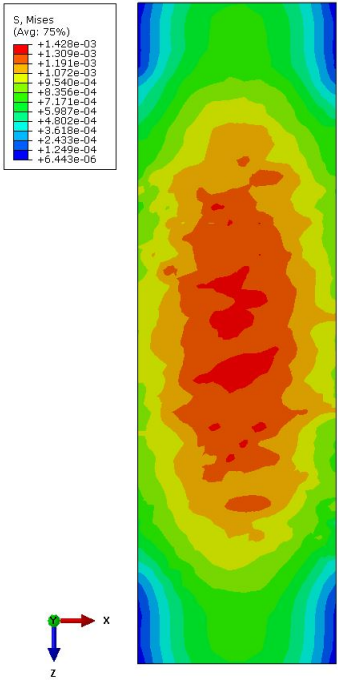


Figure 3.69: Stress distribution in the eighth ply after the curing process.

3.5 Discussion

After obtaining the numerical results from all three simulations, it is possible to evaluate the strain and stress distribution for each ply of the laminate.

The autoclave process showed high stress ($\simeq 77$ MPa) and strain concentrations in both upper and down central zones. Another important remark is the stress and strain non-uniformity, which is what mostly influences the defect appearances.

The RTM simulation was the one that showed less pronounced deformation and stress gaps through the thickness and plies of the laminate, with relatively low values ($\simeq 2$ MPa) when compared to the autoclave simulation.

Lower values of both stress and strain were tracked on the composite laminate part after performing the VBO simulation. This may be due to, when compared to the RTM, the lack of an upper mould, which eventually creates an undesirable pressure in the laminate.

Finally, comparing all the results from the different simulations, it is understandable that: i) the autoclave was the one that showed higher stress and strain concentrations through the thickness of the laminate, i.e., for the different plies. This might be due to the higher pressures that the laminate was submitted to, showing higher stress and strain gaps between distinct areas of the part; ii) both OoA processes showed a higher uniformity of the laminate in terms of strain and stress through its thickness and in an isolated ply; iii) even though the VBO simulation presented more strain concentrations than the RTM one, the strain and stress values obtained are fairly low when compared to the other two processes. Conclusively, it can be said that both of the OoA simulations revealed a lower probability of appearance of defects when compared to the autoclave one.

Chapter 4

Conclusions and Future Work

This chapter is intended to summarize the main conclusions of the thesis, as well as to recommend future work to improve the understanding of computational modelling of cure processing and defect traceability in laminated composite materials.

4.1 Conclusions

With the objective of studying the defect traceability in laminated composite materials, a finite element model was developed to represent three different manufacturing processes: autoclave, RTM and VBO.

First, a special focus was given to most of the composite materials manufacturing processes. A review of the autoclave and different open and closed moulding processes was given, emphasizing those that would be studied further and outlining some of its variants. An overview of the curing processes and types of manufacturing defects was given, followed by the explanation of the commercial of-the-shelf RAVEN[®] software.

Using RAVEN[®] software a numerical 1D analysis was performed in order to obtain the curing rate, the degree of cure and the correct value of the heat transfer coefficient that cures the composite laminate part and generates a laminate and mould temperature distribution which follows the curing temperature. This step could only be done for the autoclave and VBO processes, since the material properties of the NCF composite were obtained based on its constituents.

The heat transfer coefficient obtained for the different manufacturing composites was used as an input in the FE analysis. ABAQUS[®] software was used considering a coupled thermal-displacement step. With the correct boundary conditions, possible loads, geometries of each part, materials, interactions between parts and element types to simulate each process, it is possible to obtain the strain and stress distribution for each ply of the composite laminated part in order to know which are the most probable areas for defects to appear.

4.2 Future work

This thesis presented a development on the defect traceability of polymer composites. However, there are still developments to be made, both in terms of the FE simulation and the post processing.

Using RAVEN[®] software, it is intended to perform a representative 2D simulation in order to accurately obtain the evolution of the mechanical and thermal properties of the laminate during the cure cycle, the degree of cure, the curing rate and the glass transition temperature (T_g) by including the stiffener to the model. Thus considering a more accurate geometry of the part.

Although this thesis presented a FE thermo-expansion analysis, composite process modelling problems often involve flow compaction and a stress-deformation step. It is intended to simulate, in the future, the migration (or flow) of resin relative inside the porous medium, being the flow governed by the Darcy's law. The process induced deformations and residual stresses are meant to be simulated as well. These can be due to the mismatch of thermal-mechanical properties between the resin and the fibres, shrinkage of the resin during cure and the interaction between the part and the tool. These predictions can be used to define tool geometric compensations or to complement structural analyses.

A study on warpage prediction is also intended, particularly if the stiffener were to be manufactured in composite material, instead of steel.

Bibliography

- [1] Raju S. Davé, Markus Henne, Bryan Louis, and Paolo Ermanni. Processing: Autoclave Modeling. In Luigi Nicolais, Assunta Borzacchiello, and Stuart M. Lee, editors, Wiley Encyclopedia of Composites. John Wiley & Sons, Inc., Hoboken, NJ, USA, 2nd edition, jul 2012.
- [2] F.C. Campbell. Manufacturing Technology for Aerospace Structural Materials. Elsevier, 1st edition, 2006.
- [3] Gurit Holding AG. Guide to Composites. Available in URL: <http://www.netcomposites.com/>, 2000.
- [4] A M Waas, B V Sankar, and M W Hyer. Failure in Composites. American Society for Composites series on advances in composite materials. Destech Publications Incorporated, 2013.
- [5] S. K. Mazumdar. Composites Manufacturing. 1st edition, 2002.
- [6] Yves Béreaux, Jean-yves Charneau, Thuy Linh Pham, Jean Balcaen, Maël Moguedet, and Richard Apaloo. Plastication in injection moulding : Principles , Numerical modeling and in line Visualisation. Technical report, ALPlastics, 2013.
- [7] Mechanica Technical Solutions. Reaction Injction Molding, 2014.
- [8] Dhiren Modi. Modelling and active control of the Vacuum Infusion Process for composites manufacture. PhD thesis, University of Nottingham, 2008.
- [9] NetComposites Ltd. Resin Film Infusion, 2017.
- [10] American Composites Manufacturers Association. Composite manufacturing processes, 2016.
- [11] Suresh G. Advani and Kuang-Ting Hsiao. Manufacturing Techniques for Polymer Matrix Composites (PMCs). Woodhead Publishing Limited, 2012.
- [12] Quickstep Technologies. How The Quickstep Process Works, 2017.
- [13] Dominik Bender, Jens Schuster, and Dirk Heider. Flow rate control during vacuum-assisted resin transfer molding (VARTM) processing. Composites Science and Technology, 66(13):2265–2271, 2006.
- [14] Seemann Composites Inc. SCRIMP, 2017.

- [15] R. Chaudhari, P. Rosenberg, M. Karcher, S. Schmidhuber, P. Elsner, and F. Henning. High-Pressure RTM Process Variants for Manufacturing of Carbon Fiber Reinforced Composites. In International Conference on Composite Materials (ICCM-19), volume 3, pages 1–9, 2013.
- [16] T. Centea, L. K. Grunenfelder, and S. R. Nutt. A review of out-of-autoclave prepregs - Material properties, process phenomena, and manufacturing considerations. Composites Part A: Applied Science and Manufacturing, 70:132–154, 2015.
- [17] Bo Yang, Tianguo Jin, Fengyang Bi, Yajun Wei, and Jianguang Li. Influence of fabric shear and flow direction on void formation during resin transfer molding. Composites Part A: Applied Science and Manufacturing, 68:10–18, 2015.
- [18] Y Yang, F Robitaille, and S Hind. Thermal conductivity of carbon fiber fabrics. 19th International Conference on Composite Materials2, pages 1–10, 2013.
- [19] Saad, Miller, and Marunda. THERMAL CHARACTERIZATION OF IM7/8552-1 CARBON-EPOXY COMPOSITES Messiha. pages 1–8, 2017.
- [20] H. Molker, D. Wilhelmsson, Renaud Gutkin, and Leif E. Asp. Orthotropic criteria for transverse failure of non-crimp fabric-reinforced composites. Journal of Composite Materials, 50(18):2445–2458, 2015.
- [21] Cecen, Tavman, Kok, and Aydogdu. Epoxy- and Polyester-Based Composites Reinforced With Glass, Carbon and Aramid Fabrics: Measurement of Heat Capacity and Thermal Conductivity of Composites by Differential Scanning Calorimetry. Polymers and Polymer Composites, 16(2):101–113, 2008.
- [22] R. McIlhagger, J. P. Quinn, A. T. McIlhagger, S. Wilson, D. Simpson, and W. Wenger. The influence of binder tow density on the mechanical properties of spatially reinforced composites. Part 2 - Mechanical properties. Composites Part A: Applied Science and Manufacturing, 39(2):334–341, 2008.
- [23] David Van Ee and Anoush Poursartip. NCAMP Hexply Material Properties Database for use with COMPRO CCA and Raven. National Center for Advanced Materials Performance, page 141, 2009.
- [24] Hexcel. HexPly ® 8552 - Product Data Sheet - EU Version. pages 1–6, 2016.
- [25] Cytec Engineered Materials. CYCOM 5320 toughened epoxy for structural applications, out-of-autoclave manufacturing. Information Sheet, 324(October):1–11, 2015.
- [26] Cytec. AEROSPACE MATERIALS CYCOM ® 890 RTM Resin System. Technical Data Sheet, (August 2010), 2013.
- [27] High Temp Metals. INVAR 36® TECHNICAL DATA, 2015.
- [28] Seong Hwan Yoo, Min Gu Han, Jin Ho Hong, and Seung Hwan Chang. Simulation of curing process of carbon/epoxy composite during autoclave degassing molding by considering phase changes of epoxy resin. Composites Part B: Engineering, 77:257–267, 2015.

- [29] Shu Minakuchi, Shoma Niwa, Kazunori Takagaki, and Nobuo Takeda. Composite cure simulation scheme fully integrating internal strain measurement. Composites Part A: Applied Science and Manufacturing, 84:53–63, 2016.
- [30] S R White and H T Hahn. Process Modeling of Composite Materials: Residual Stress Development during Cure: Part I - Model Formulation. Journal of Composite Materials, 26(16):2402–2422, 1992.
- [31] S R White and H T Hahn. Process Modeling of Composite Materials: Residual Stress Development during Cure: Part II - Experimental Validation. Journal of Composite Materials, 1992.
- [32] V. A F Costa and A. C M Sousa. Modeling of flow and thermo-kinetics during the cure of thick laminated composites. International Journal of Thermal Sciences, 42(1):15–22, 2003.
- [33] A. S. Ganapathi, Sunil C. Joshi, and Zhong Chen. Simulation of bleeder flow and curing of thick composites with pressure and temperature dependent properties. Simulation Modelling Practice and Theory, 32:64–82, 2013.
- [34] Gasser F. Abdelal, Antony Robotham, and Wesley Cantwell. Autoclave cure simulation of composite structures applying implicit and explicit FE techniques. International Journal of Mechanics and Materials in Design, 9(1):55–63, 2013.
- [35] Thammaiah Sreekantamurthy, Tyler B Hudson, Tan-Hung Hou, and Brian W Grimsley. Composite Cure Process Modeling and Simulations using COMPRO[®] and Validation of Residual Strains using Fiber Optics Sensors. In 31st ASC technical conference, 2016.
- [36] F. Trochu, R. Gauvin, and D. Gao. Numerical Analysis of the Resin Transfer Molding Process by the Finite Element Method. Welding Research, 91(2):270–277, 2012.
- [37] Baichen Liu, Simon Bickerton, and Suresh G. Advani. Modelling and simulation of resin transfer moulding (RTM) - Gate control, venting and dry spot prediction. Composites Part A: Applied Science and Manufacturing, 27(2):135–141, 1996.
- [38] F R Phelan. Simulation of the injection process in resin transfer molding. Polymer Composites, 18(4):460–476, 1997.
- [39] Cheng Tan and George Springer. Composite Manufacturing: Simulation of 3-D Resin Transfer Moulding. Journal of Composite Materials, Vol. 33(No. 18/1999):1716–1742, 1999.
- [40] Z Dimitrovová and L Faria. Finite element modeling of the resin transfer molding process based on homogenization techniques. Computers & Structures, 76(1-3):379–397, 2000.
- [41] David Rouison, M. Sain, and M. Couturier. Resin transfer molding of natural fiber reinforced composites: Cure simulation. Composites Science and Technology, 64(5):629–644, 2004.

- [42] Q. Govignon, S. Bickerton, and P. A. Kelly. Simulation of the reinforcement compaction and resin flow during the complete resin infusion process. Composites Part A: Applied Science and Manufacturing, 41(1):45–57, 2010.
- [43] Geneviève Palardy, Pascal Hubert, Eduardo Ruiz, Mohsan Haider, and Larry Lessard. Numerical simulations for class A surface finish in resin transfer moulding process. Composites Part B: Engineering, 43(2):819–824, 2012.
- [44] T. L. Anderson. Fracture Mechanics: Fundamentals and Applications, volume 58. 2012.
- [45] Plastics Alchemy - Recycling. Chemistry World, 2005.
- [46] Saravanan Rajendran, Lino Scelsi, Alma Hodzic, Constantinos Soutis, and Mariam A. Al-Maadeed. Environmental impact assessment of composites containing recycled plastics. Resources, Conservation and Recycling, 60:131–139, 2012.
- [47] James C Seferis, Roman W Hillermeier, and FrÉDÉRIC U Buehler. Prepregging and Autoclaving of Thermoset Composites. In Anthony Kelly and Carl Zweben, editors, Comprehensive Composite Materials, chapter 2.20, pages 701–736. Elsevier Ltd, 2000.
- [48] Laraib Khan, Wajid Khan, and S. Ahmed. Out-of-Autoclave (OOA) Manufacturing Technologies for Composite Sandwich Structures. In Raja Das and Mohan Pradhan, editors, Handbook of Research on Manufacturing Process Modeling and Optimization Strategies, chapter Chapter 14, pages 292–317. IGI Global, 2017.
- [49] Nuno Correia. Analysis of the Vacuum Infusion Moulding Process. PhD thesis, University of Nottingham, 2004.
- [50] Hugo Faria. Analytical and Numerical Modelling of the Filament Winding Process. PhD thesis, Universidade do Porto, 2013.
- [51] A.K. Kulshreshtha. Handbook of Polymer Blends and Composites, Volume 2. In A.K. Kulshreshtha and Cornelia Vasile, editors, Handbook of Polymer Blends and Composites, volume 2, page 428. Rapra Technology Limited, 2002.
- [52] A. Brent Strong. Fundamentals of Composites Manufacturing Materials, Methods, and Applications. Society of Manufacturing Engineers, Dearborn, Michigan, 2nd edition, 2008.
- [53] Goodwinds Composites. Roll wrapping, 2011.
- [54] Composites One. Process, 2017.
- [55] Gardner Business Media Inc. Resin infusion processes, 2007.
- [56] Owens Corning Composite Materials LLC. Processes, 2017.
- [57] Exel Group World Wide. Continuous Lamination, 2009.

- [58] Jawad Ahmad Nisar. Modelling the interfaces of bondable pultrusions. PhD thesis, University of Glasgow, 2010.
- [59] N. K. Naik, M. Sirisha, and A. Inani. Permeability characterization of polymer matrix composites by RTM/VARTM. Progress in Aerospace Sciences, 65:22–40, 2014.
- [60] C Ridgard. Out of Autoclave Composite Technology for Aerospace, Defense and Space Structures. In International Sampe Symposium and Exhibition, page 163. Society for the Advancement of Material and Process Engineering, 2009.
- [61] Mathieu Préau. Defect Management in Vacuum Bag Only Semipreg Processing of Co-bonded Composite Repairs. PhD thesis, McGill University, 2016.
- [62] Timotei Centea and Steven R Nutt. Manufacturing cost relationships for vacuum bag-only prepreg processing. Journal of Composite Materials, 50(17):2305–2321, 2016.
- [63] Crystic. Composites Handbook - Performance Resins in Composites. Scott Bader Group of Companies Scott, 2005.
- [64] B de Parscau du Plessix, S le Corre, F Jacquemin, P Lefebure, and V Sobotka. Improved simplified approach for the prediction of porosity growth during the curing of composites parts. Composites Part A, 90:549–558, 2016.
- [65] Xueshu LIU and Fei CHEN. A review of void formation and its effects on the mechanical performance of carbon fibre reinforced plastic. Engineering Transactions, 64(1):33–51, 2016.
- [66] L K Grunenfelder and S R Nutt. Void formation in composite prepreps – Effect of dissolved moisture. Composites Science and Technology, 70(16):2304–2309, 2010.
- [67] Composites Science, Edu Ruiz, Polytechnique Montr, Sofiane Soukane, Ecole Nationale Sup, Francois Trochu, Polytechnique Montr, and Flexible Injection View. Optimization of injection flow rate to minimize micro / macro-voids formation in resin transfer molded composites Optimization of injection flow rate to minimize micro / macro-voids formation in resin transfer molded composites. Composites Science and Technology, 66:475–486, 2006.
- [68] Bijoy Sri Khan, Kevin D Potter, and Michael R Wisnom. Simulation of process induced defects in resin transfer moulded woven carbon fibre laminates and their effect on mechanical behaviour. In The 8th International Conference on Flow Processes in Composite Materials (FPCM8), number 11, pages 261–270, 2006.
- [69] G. Fernlund, N. Rahman, R. Courdji, M. Bresslauer, A. Poursartip, K. Willden, and K. Nelson. Experimental and numerical study of the effect of cure cycle, tool surface, geometry, and lay-up on the dimensional fidelity of autoclave-processed composite parts. Composites - Part A: Applied Science and Manufacturing, 33(3):341–351, 2002.

- [70] M. R. Wisnom, M. Gigliotti, N. Ersoy, M. Campbell, and K. D. Potter. Mechanisms generating residual stresses and distortion during manufacture of polymer-matrix composite structures. Composites Part A: Applied Science and Manufacturing, 37(4):522–529, 2006.
- [71] Jun Li, Xuefeng Yao, Yinghua Liu, Zhangzhi Cen, Zhejun Kou, and Di Dai. A study of the integrated composite material structures under different fabrication processing. Composites Part A: Applied Science and Manufacturing, 40(4):455–462, 2009.
- [72] K Cinar, N B Ersoy, and F E Oz. 3D Process Modelling for Distortions in Manufacturing of Polymer Composite Materials. In ECCM15, pages 24–28, 2012.
- [73] Amandeep Sivia, Jaspalpreet Grewal, Amritpal Bhinder, and Rajkamal Saini. A Study on the Skin-Stringer Panel of an Aircraft. 1(1):40–44, 2014.
- [74] J. A. Barnes, I. J. Simms, G. J. Farrow, D. Jackson, G. Wostenholm, and B. Yates. Thermal expansion characteristics of PEEK composites. Journal of Materials Science, 26(8):2259–2271, 1991.
- [75] Columbia Metals. Controlled Expansion Alloys. 36.
- [76] Paul Walsh. Comparison of Invar and Composite Tooling Materials for Precision Composite Part Manufacture. (October), 2015.
- [77] Steven L Abberger. Invar Truths and Rumors 2 . 0. page 9, 2013.
- [78] Thammaiah Sreekantamurthy, Tyler B Hudson, Tan-Hung Hou, and Brian W Grimsley. Composite Cure Process Modeling and Simulations using COMPRO[®] and Validation of Residual Strains using Fiber Optics Sensors. 31st ASC technical conference, 2016.
- [79] Convergent Manufacturing Technologies. Compro modelling guidelines, 2016.

Appendix A

ABAQUS[®] 3D computational models

Appendix A contains the *.cae* and *.jnl* of the three different manufacturing computational processes studied, i.e. autoclave, RTM and VBO.

The description of each of the computational models is given in Section 3.4.

A folder named "Models" with the files can be found on the CD attached.